Atmos. Chem. Phys., 11, 10853–10870, 2011
www.atmos-chem-phys.net/11/10853/2011/
doi:10.5194/acp-11-10853-2011

Atmospheric Chemistry and Physics

Variable lifetimes and loss mechanisms for NO_3 and N_2O_5 during the DOMINO campaign: contrasts between marine, urban and continental air

J. N. Crowley[1], J. Thieser[1], M. J. Tang[1], G. Schuster[1], H. Bozem[1], Z. H. Beygi[1], H. Fischer[1], J.-M. Diesch[2], F. Drewnick[2], S. Borrmann[2,3], W. Song[1], N. Yassaa[1,4], J. Williams[1], D. Pöhler[5], U. Platt[5], and J. Lelieveld[1]

[1]Max-Planck-Institut für Chemie, Division of Atmospheric Chemistry, Mainz, Germany
[2]Max-Planck-Institut für Chemie, Particle Chemistry Department, Mainz, Germany
[3]Institute for Atmospheric Physics, University of Mainz, Germany
[4]Faculty of Chemistry, University of Sciences and Technology Houari Boumediene (USTHB), Algiers, Algeria
[5]Institut of Environmetal Physics, University of Heidelberg, Germany

Received: 8 June 2011 – Published in Atmos. Chem. Phys. Discuss.: 23 June 2011
Revised: 22 September 2011 – Accepted: 4 October 2011 – Published: 3 November 2011

Abstract. Nighttime mixing ratios of boundary layer N_2O_5 were determined using cavity-ring-down spectroscopy during the DOMINO campaign in Southern Spain (Diel Oxidant Mechanisms In relation to Nitrogen Oxides, 21 November 2008–8 December 2008). N_2O_5 mixing ratios ranged from below the detection limit (∼5 ppt) to ∼500 ppt. A steady-state analysis constrained by measured mixing ratios of N_2O_5, NO_2 and O_3 was used to derive NO_3 lifetimes and compare them to calculated rates of loss via gas-phase and heterogeneous reactions of both NO_3 and N_2O_5. Three distinct types of air masses were encountered, which were largely marine (Atlantic), continental or urban-industrial in origin. NO_3 lifetimes were longest in the Atlantic sector (up to ∼30 min) but were very short (a few seconds) in polluted, air masses from the local city and petroleum-related industrial complex of Huelva. Air from the continental sector was an intermediate case. The high reactivity to NO_3 of the urban air mass was not accounted for by gas-phase and heterogeneous reactions, rates of which were constrained by measurements of NO, volatile organic species and aerosol surface area. In general, high NO_2 mixing ratios were associated with low NO_3 lifetimes, though heterogeneous processes (e.g. reaction of N_2O_5 on aerosol) were generally less important than direct gas-phase losses of NO_3. The presence of SO_2 at levels above ∼2 ppb in the urban air sector was always associated with very low N_2O_5 mixing ratios indicating either very short NO_3 lifetimes in the presence of combustion-related emissions or an important role for reduced sulphur species in urban, nighttime chemistry. High production rates coupled with low lifetimes of NO_3 imply an important contribution of nighttime chemistry to removal of both NO_x and VOC.

Correspondence to: J. N. Crowley
(john.crowley@mpic.de)

1 Introduction

The photochemically driven, OH-initiated oxidation processes during the day are supplemented by (or, for several classes of volatile organic compounds (VOCs) such as terpenes or CH_3SCH_3, surpassed by) night-time reactions with the NO_3 radical (Wayne et al., 1991). The interaction of NO_3 with VOCs leads to the formation of organic peroxy radicals, and via secondary reactions to HO_2 and OH (Platt et al., 1990; Sommariva et al., 2009). NO_3 can thus initiate and propagate nocturnal radical chemistry linking HO_2 and NO_x chemistry and significantly impacting on oxidation rates of several classes of atmospheric traces gases.

NO_3 is formed predominantly in the reaction of NO_2 with O_3 (Reaction R1) and is converted to N_2O_5 via further reaction with NO_2 (Reaction R2). The thermal decomposition of N_2O_5 links the concentrations of NO_3 and N_2O_5 via the equilibrium constant, $K3$. Simultaneous measurements of NO_3 and N_2O_5 (Brown et al., 2003a; Crowley et al., 2010) confirm that (under most conditions) the timescales to acquire equilibrium are sufficiently short that the relative concentrations of NO_3 and N_2O_5 in the atmosphere are controlled only by the temperature and levels of NO_2.

$$NO_2 + O_3 \rightarrow NO_3 + O_2 \quad \text{(R1)}$$

$$NO_2 + NO_3 + M \rightarrow N_2O_5 + M \quad \text{(R2)}$$

$$N_2O_5 + M \rightarrow NO_2 + NO_3 + M \quad \text{(R3)}$$

The impacts of NO_3 and N_2O_5 on nighttime chemistry depends on their relative rates of loss via gas-phase and heterogeneous reactions. Whereas NO_3 is lost mainly via gas-phase reactions with e.g. VOCs (see above), N_2O_5 is removed predominantly by heterogeneous hydrolysis on aqueous aerosol, which can substantially modify the amount of reactive nitrogen available for daytime photochemistry. In the polluted boundary layer, this process influences the fate of NO_x emissions and their potential for photochemical ozone formation and also (via heterogeneous chemistry on sulphate particles) links O_3 production rates to emissions of SO_2 from e.g. power plants or shipping (Brown et al., 2006). It has recently been shown that heterogeneous reactions of N_2O_5 with chloride containing particles can also represent a significant source of photo-labile chlorine (in the form of $ClNO_2$ and Cl_2) (Roberts et al., 2009; Thornton et al., 2010).

The objectives of this study were to examine the roles and relative importance of gas phase and heterogeneous processing of NO_3 and N_2O_5 in chemically distinct air masses: urban (strong anthropogenic influence), continental (mainly biogenic emissions) and maritime. In order to achieve these objectives the NO_3 and N_2O_5 measurements were accompanied by instrumentation for trace gas and aerosol characterisation (see later).

1.1 NO_3 lifetimes

The production rate of NO_3 is given by $k_1\,[NO_2][O_3]$ (generally we write k_i as the rate coefficient for Reaction Ri) so that its stationary state turnover lifetime, $\tau_{ss}(NO_3)$, can be calculated from observations of its concentration and those of O_3 and NO_2:

$$\tau_{ss}(NO_3) = \frac{[NO_3]}{k_1[NO_2][O_3]} \quad (1)$$

Whenever we use the term "NO_3 lifetimes" in the manuscript, we refer to $\tau_{ss}(NO_3)$.

NO_3 can be removed directly from the air by e.g. reaction with organic trace gases (Wayne et al., 1991) or indirectly via removal of N_2O_5 via e.g. heterogeneous loss to aqueous particles. As described previously (Geyer et al., 2001b; Aldener et al., 2006; Crowley et al., 2010) the contributions of direct and indirect losses of NO_3 to its lifetime can, in principal, be evaluated if K_2 (the equilibrium constant k_2/k_3) and $[NO_2]$ are known:

$$\tau_{ss}(NO_3) \approx \frac{1}{f_{ss}(NO_3)} \quad (2)$$

where $f_{ss}(NO_3)$ is the overall loss frequency of NO_3 from stationary state and is equal to

$$\sum_i (k_i[X]_i) + 0.25\bar{c}\gamma(NO_3)A + f_{dd}(NO_3)$$

$$+\left(0.25\bar{c}\gamma(N_2O_5)A + f_{dd}(N_2O_5) + f_{H_2O}\right)K_2[NO_2]$$

In this expression, k_i (cm^3 molecule $^{-1}$ s^{-1}) is the rate coefficient for reaction of NO_3 with trace gas i at concentration $[X]_i$ (molecule cm^{-3}), A is the aerosol surface area density (cm^2 cm^{-3}), $\bar{c}$ ($cm\,s^{-1}$) is the mean molecular velocity of NO_3 or N_2O_5, $\gamma(NO_3)$ and $\gamma(N_2O_5)$ are the dimensionless uptake coefficients for irreversible reaction of NO_3 or N_2O_5 with aerosol, f_{dd} (s^{-1}) is the first-order rate constant for dry deposition of NO_3 or N_2O_5 and f_{H_2O} (s^{-1}) represents the homogeneous, gas-phase loss of N_2O_5 via reaction with water vapour.

Recent measurements of long lifetimes of N_2O_5 even in the presence of high relative humidity (Brown et al., 2009; Crowley et al., 2010) imply that f_{H_2O} is too small to be important under most conditions. The rate of uptake of a trace gas to airborne particles can be reduced by concentration gradients close to the particle surface, which requires modification of the simple expression for the heterogeneous loss rate, $k_{het} = 0.25\bar{c}\gamma A$, as used in Eq. (2). The effective uptake coefficient ($\gamma_{effective}$) is approximated by (Fuchs and Sutugin, 1970):

$$\frac{1}{\gamma_{effective}} = \frac{1}{\gamma} + \frac{0.75 + 0.283Kn}{Kn(Kn+1)} \quad (3)$$

where $Kn = \frac{3D_g}{\bar{c}\cdot r_{sw}}$, r_{sw} is the radius of the particle at the maximum of the surface area weighted size distribution, and D_g is the gas phase diffusion coefficient of N_2O_5 or NO_3 at the appropriate pressure and temperature. For N_2O_5, D_g is $0.085\,cm^2$ s^{-1} at atmospheric pressure and 298 K (Wagner et al., 2008). During the nights of the campaign, the dominant contribution to aerosol surface area was by particles with diameters of less than ~200 nm. In this case, only uptake coefficients close to unity require significant correction. For example, an uptake coefficient of ~0.1 would be reduced by transport limitations to ~0.09, whereas a γ of 1 would reduce to ~0.5. A value of 0.5 is therefore the approximate maximum value of $\gamma(N_2O_5)$ or $\gamma(NO_3)$, which can be used to calculate NO_3 lifetimes using Eq. (2). More realistic (lower) values of γ, derived from laboratory and field experiments are discussed later. At low aerosol loading (or low values of γ) and negligible dry deposition the term (in Eq. 2) $(0.25\bar{c}\gamma(N_2O_5)A + f_{dd}(N_2O_5) + f_{H_2O}K_2[NO_2])$ becomes diminishingly small and NO_3 lifetimes are largely independent of NO_2 concentrations. On the other hand, if gas-phase losses of NO_3 are slow, N_2O_5 chemistry can be important and NO_3 lifetimes will show a dependence on the inverse NO_2 concentration (Heintz et al., 1996; Martinez et al., 2000; Geyer et al., 2001b; Brown et al., 2003a, b, 2009; Aldener et al., 2006).

Certain conditions must be fulfilled if Eq. (2) is used to examine NO_3 lifetimes and draw conclusions regarding direct

and indirect loss routes. Firstly, NO_3 production rates are governed by a slow reaction between NO_2 and O_3. Application of a stationary state analysis to NO_3 lifetimes is only suited to air-masses where the chemical lifetime of NO_3 (or N_2O_5) is sufficiently short that stationary state is achieved with the transport time from the emission region to the measurement site (Brown et al., 2003a).

Stationary state is formally achieved when the rate of change of NO_3 and N_2O_5 are zero, i.e. $dNO_3/dt = k_1[NO_2][O_3] + k_3[N_2O_5] - k_2[NO_2][O_3] - k'(NO_3)[NO_3] = 0$ and $dN_2O_5/dt = k_2[NO_2][NO_3] - k_3[N_2O_5] - k''[N_2O_5] = 0$, where $k'(NO_3)$ and $k''(N_2O_5)$ are summed first order loss rate constants for any reactions involving NO_3 and N_2O_5. The approximate time to achieve stationary state thus depends on the production and loss rates of both NO_3 and N_2O_5 and is longer at high NO_2 mixing ratio and low temperatures.

Time dependent values of dNO_3/dt and dN_2O_5/dt were determined for an unfavourable case (i.e. high NO_2 mixing ratio of 10 ppb) by numerical simulation in a manner similar to that described previously (Brown et al., 2003a). The low N_2O_5 and NO_3 concentrations observed (implying short lifetimes) meant that stationary state was achieved within 1–2 h after dusk and within the time of transport from the major source of NO_x (e.g. Huelva).

Equation (2) has been used to derive the direct and indirect contributions to NO_3 loss rates (Brown et al., 2009; Crowley et al., 2010) via the dependence of the observed lifetime on NO_2 mixing ratios. This approach will however break down if the trace gases which react directly with NO_3 are correlated (e.g. have the same chemical source or spatial distribution of emissions) with NO_2. This is unlikely to apply to regions where NO_3 losses are dominated by e.g. reaction with biogenic volatile organic compounds (BVOC) in clean air masses, but might be the case where NO_3 reacts with traces gases resulting from combustion processes in which NO_2 is also generated. In a similar vein, if aerosol surface area also co-varies with NO_2, use of Eq. (2) to separate the contributions of homogeneous and heterogeneous loss rates of N_2O_5 to the NO_3 lifetime is not possible.

2 Site description

The DOMINO campaign (Diel Oxidant Mechanisms In relation to Nitrogen Oxides, (21 November 2008–8 December 2008) took place at the Atmospheric Sounding Station (Base de Arenosillo[1], 37°05′58″ N, 6°44′17″ W) located on the Atlantic coast of the southern Spanish region of Moguer (Fig. 1). Measurements were conducted in a forested area (mainly Stone pines, *Pinus pinea* ∼5–10 m in height) with

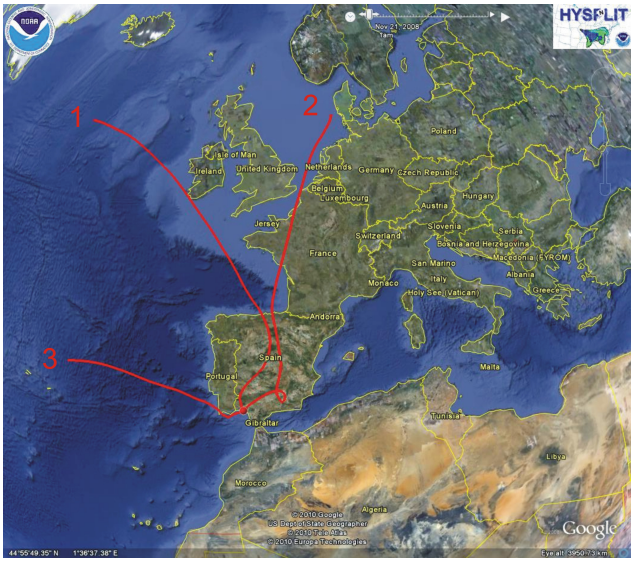

Fig. 1. Location of the measurement site with three 72 h HYSPLIT back-trajectories of air masses reaching the site at 00:00 on the 24 November 2008 (1, Huelva sector), 27 November 2008 (2,continental sector) and 7 December 2008 (3, Atlantic sector).

proximity to both extensive pollution sources and the Atlantic Ocean (the Atlantic coast was ∼300 m distant and ∼20 m lower) so that the chemical composition of air masses arriving at the site was highly dependent on wind direction. On-site wind directions between 290 and 340 degrees indicated that air masses had recently passed over the expansive industrial centre and port of Huelva (henceforth referred to as the "Huelva" sector) which was located about 30 km away, or with typical night-time wind-speeds of 8–18 km h^{-1} about 2–3 h upwind. Huelva houses one of Europe's larger oil refineries and pollution from this sector includes emissions from related industrial/shipping activity. Air from the Huelva sector arriving at the measurement site at night was frequently and strongly malodorous. Air arriving from the 150–270 degrees sector passed over the Atlantic (sector "Atlantic") and generally contained low levels of NO_x. NO_2 plumes were occasionally observed in this sector, which were usually accompanied by enhanced levels of SO_2 indicating emissions from passing ships.

Wind directions between 0 and 45 degrees (sector "continental") were from mainland Spain and passed no large cities for several hours prior to arrival at the site. Air arriving from Sevilla (∼60 degrees), following Huelva, the next largest potential source of pollutants, was rarely encountered during the night. Overall, during the nights of the campaign, the air arrived predominantly from the Huelva (∼50 %) or continental sectors (∼35 %), with air from the Atlantic sector (∼15 %) encountered less frequently. Air mass back-trajectories calculated using HYSPLIT with GDAS meteorology (Draxler and Rolph, 2011) confirmed the allocation

[1]El Arenosillo is a platform of the Atmospheric Research and Instrumentation Branch of the Spanish National Institute for Aerospace Technology (INTA) dedicated to atmospheric measurements in the Southwest of Spain.

of source region sector according to local wind directions. Figure 1 displays selected back-trajectories for air arriving at midnight from the Huelva sector (1), the continental sector (2) and the Atlantic sector (3).

3 Methods

3.1 NO_3 and N_2O_5

NO_3 and N_2O_5 mixing ratios were measured using a two-channel, off axis cavity-ring-down system (OA-CRD), which has recently been described in detail (Schuster et al., 2009; Crowley et al., 2010) and also by long-path, differential optical absorption spectroscopy (LP-DOAS). In the CRD instrument, one channel monitors NO_3 directly, the other is used to monitor the sum of NO_3 and N_2O_5 via thermal dissociation of N_2O_5. The instrument was located in the upper container of a two-container stack and sampled air through a few meters of 1/4 or 1/2″ PFA-tubing with the inlet sampling from a height of between 7 and 12 m above ground level (∼1–5 m above the closest canopy).

The 1/2″ inlet was operated with a large bypass flow to reduce the residence time. A 2 µm pore Teflon filter (replaced every hour) in a PFA filter holder was located at the end of the inlet outside the container. The losses of NO_3 and N_2O_5 to the filter (15 ± 3 % and <2 %, respectively) were characterised prior to and after the campaign. Loss rates in the Teflon coated (DuPont, FEP) glass cavities were also measured during the campaign. Operational pressures and flows resulted in residence times in the inlet lines and cavities of between 0.6 and 1 s. CRD noise-levels changed during the campaign and varied between ∼3 and 7 pptv for N_2O_5 and between 2 and 5 pptv for NO_3 (both with 5 s integration per datapoint). The detection limit is partly defined by accuracy of the chemical zero (measured by adding NO as described in detail previously (Schuster et al., 2009) and was between 2 and 3 pptv for NO_3 and 5–7 pptv for N_2O_5 (both assuming zero losses in the inlet tubing). However, NO_3 was not observed directly during the campaign even when N_2O_5 levels of several hundred pptv were present. As NO_2 levels were not sufficiently high and temperatures (controlling K_2) not sufficiently low to reduce NO_3 to below the detection limit, this indicates deviation of the NO_2-NO_3-N_2O_5 chemistry from equilibrium. With night-time temperatures occasionally as high as 15 °C, equilibrium should be established within in a few minutes, suggesting that any processes that rapidly drain NO_3 from equilibrium must be very local otherwise N_2O_5 would also have been completely removed.

A potential cause of dis-equilibrium between NO_2, O_3 and N_2O_5 is the loss of NO_3 in the PFA inlet. This had not been anticipated as it was not encountered on a previous campaign at a rural location (Crowley et al., 2010) in which a similar sampling strategy (long PFA line with 1 s residence time) had been periodically deployed in place of the normally used, FEP-coated high-volume flow glass sampling line. Use of new inlet lines did not result in observation of NO_3, even temporarily. On several occasions during the campaign a calibration source of NO_3 was added to the inlet to measure its transmission and also that of the NO_3 cavity. NO_3 was generated by the thermal decomposition (∼90 °C) of N_2O_5, itself made by mixing NO_2 and O_3 in a blackened, FEP-coated glass reaction vessel as described previously (Schuster et al., 2009). Prior to heating, the mixture typically contained approximately 200–400 pptv N_2O_5, 150 ppbv O_3 and 5 ppbv NO_2. The results were rather surprising as the initial transmission of the inlet tubing to NO_3 was very low (on occasions less than 20 %) even if it was relatively fresh. The transmission increased with exposure to the O_3, NO_2, NO_3 mixture to a value (circa 70–80 %) commensurate with known loss rates of NO_3 in PFA tubing. This condition sometimes took as long as an hour to achieve. At the same time, loss rates of NO_3 in the cold cavity were recorded as high as $1\,s^{-1}$, a factor 5 larger than observed in the laboratory, whereas loss in the hot cavity (i.e. the $N_2O_5 + NO_3$ channel) proceeded at the usual rate ($\sim 0.2\,s^{-1}$). These observations indicate that the PFA tubing rapidly became reactive to NO_3 when exposed to the air and this reactivity could be reduced by extended passivation with high NO_3/O_3 concentrations or by heating to 90 °C. Post-campaign tests of the inlets used also revealed high (initial) reactivity to NO_3.

Assuming that the loss of NO_3 occurred in our inlet, it took place on a timescale (1 s) which is considerably shorter than the thermal lifetime of N_2O_5 (minutes), so that the N_2O_5 mixing ratios would not have been significantly affected. In this case we can calculate NO_3 ambient mixing ratios from the measured N_2O_5 and NO_2 and the equilibrium constant, K_2 via (Eq. 4).

$$[NO_3] = \frac{[N_2O_5]}{K_2[NO_2]} \quad (4)$$

As the inlet tubing was protected with a Teflon filter we do not anticipate large losses of N_2O_5 due to coating of the wall with aerosol. The disadvantage with this indirect calculation of NO_3 is that it relies on high quality (accurate, low noise), and preferably high time resolution NO_2 measurements. Some uncertainty is also associated with K_2, though recent field measurements of NO_2, NO_3 and N_2O_5 suggest that this is not more than 20 % (Osthoff et al., 2007; Crowley et al., 2010). The uncertainty in NO_3 mixing ratios calculated this way is thus considerably larger than via direct measurements and are estimated as about 35 % if $N_2O_5 < 7$ ppt. At lower levels of N_2O_5 the uncertainty in N_2O_5 (∼40 % at 5 ppt) dominates. Long-path differential optical absorption spectroscopy (LP-DOAS, see below) measurements of NO_3 taken at a similar height to the CRD inlet are however in good agreement with the CRD-NO_3 mixing ratios derived from N_2O_5 and NO_2.

The LP-DOAS instrument applies the set-up from Merten et al. (2011) with a configuration described in Pöhler et al. (2010). It uses a telescope of 1.5 m focal length a 100 or 200 µm fibre bundle a 75 W XBO xenon arc lamp (Osram) and for spectral analysis an Acton 300 i spectrometer with Roper Scientific CCD camera (Spec-10:2KBUV). The instrument was located at 9 m above the ground about 800 m north of the main sampling point. It was operated with three sets of retro-reflectors mounted on a tower at 20, 35 and 70 m above the ground at a distance of 4.8 km to the east, resulting in a total optical path-length of 9.6 km. The data analysis of NO_3 was performed in the spectral range from 615.0 nm to 673.8 nm with a gap between 644.1 nm to 657.8 nm to avoid strong water absorption lines. The reference spectra used were: NO_3 (Yokelson et al., 1994), NO_2 (Vandaele et al., 1998), O_3 (Voigt et al., 2001), H_2O (Hitran 2006 from Gordon et al., 2007) and additionally a recorded spectrum at noon to correct for most H_2O absorption, a background spectrum and a 3rd order polynomial. The standard deviation σ of the measurements was estimated according to Stutz and Platt (1996) and resulted in an average uncertainty for the NO_3 mixing ratio of 1 ppt. In this work we use data at from the lowest retro reflector only in order to compare with the CRD measurements.

3.2 NO_2 and NO

NO and NO_2 measurements were made with a modified commercial chemiluminescence detector (CLD 790 SR) originally manufactured by ECO Physics (Duernten, Switzerland). The quantitative detection of NO_2 is based on its photolytic conversion (Blue Light Converter, Droplet Measurement Technologies, Boulder, Co, USA) to NO, which was subsequently detected in the CLD (Kley and McFarland, 1980). The detection limits for the NO and NO_2 measurements were 6 pptv and 8 ppt, respectively for an integration period of 1 s. The total uncertainties for the measurements of NO, NO_2 were determined both to be 10 %, based on the reproducibility of in-field background measurements, calibrations, the uncertainties of the standards and the conversion efficiency of the photolytic converter. The drift in instrument zero was less than ∼2 ppt over the duration of one night. The same device was described in more detail recently (Crowley et al., 2010).

3.3 O_3, SO_2 and H_2O

O_3 and SO_2 (Airpointer, Recordum GmbH) and H_2O (LICOR 840 gas analyser, LI-COR, Inc.) were measured using instrumentation onboard the MoLa mobile platform (Diesch et al., 2011). Limits of detection and precision were 0.5 ppb and 1 ppb for both SO_2 and O_3, 0.4 ppb and 1 ppb for NO_x. Whilst Airpointer measurements of NO and NO_2 mirrored the trends seen using the ECO Physics device described above, they were not sufficiently accurate (especially at low NO_x levels) to perform NO_3 lifetime analyses.

3.4 Volatile organic compounds

A commercially available instrument (AERO Laser model AL 4021, Germany) was used for in-situ HCHO measurements. This instrument is based on the Hantzsch reagent method, following the design described in Kelly and Fortune (1994). The time resolution is 160 s. Detection limit and precision were estimated from the 1σ-reproducibility of in-situ zero and calibration gas measurements as 22 pptv and ±15 %, respectively. The total uncertainty is estimated to be 29 %. An on-line sampling Thermal Desorption-Gas Chromatograph-Mass Spectrometer (TD-GC-MS) measurement system was used for the in-situ observation of anthropogenic VOCs such as ethylbenzene, and all xylene isomers as well as biogenic species such as isoprene and monoterpenes (Song et al., 2011). C_1–C_4 alkenes and alkanes were not measured.

3.5 Aerosol measurements

Particle size information was obtained using MoLa instruments (see above). A Fast Mobility Particle Sizer (FMPS 3091, TSI, Inc.), an Aerodynamic Particle Sizer (APS 3321, TSI, Inc.) as well as an Optical Particle Counter (OPC 1.109, Grimm) covered a particle size range from 5.6 nm to 32 µm. The chemical composition of the non-refractory aerosol in the sub-micron range was measured by means of a High-Resolution-Time-of-Flight Aerosol Mass Spectrometer (HR-ToF-AMS, Aerodyne Res., Inc.). The soot (black carbon) concentration in PM_1 was determined by a Multi Angle Absorption Photometer (MAAP, Thermo E.C.). The aerosol surface area (ASA) used for calculating rates of trace gas uptake was calculated only from the FMPS dataset as, for most nights (including those examined in detail later), this contributed ≥80 % of the total aerosol surface area and (in contrast to super-micron particles) was of known composition.

3.6 Meteorological parameters

Wind direction and speed, temperature and pressure and relative humidity and rain intensity at approximate inlet height were provided by MoLa instrumentation (WXT 510 weather station, Vaisala). Temperatures and wind directions were also available at heights of 25, 50 and 100 m from a local meteorological tower operated by INTA.

Several cloudless nights gave rise to a strong temperature inversion, with temperatures at a height of 100 m up to 5–6 °C warmer than those measured at the inlet height (∼10 m). This inversion would have lead to a very stable nocturnal boundary layer with efficient accumulation of low altitude emissions from e.g. the Huelva industrial area.

4 Measurements and discussion

Measurements of N_2O_5 and NO_3 were made on all campaign nights with the exception of 28–29 November. N_2O_5 was observed on most nights, though it was never present above the detection limit throughout the night but rather appeared in bursts of a few hours duration, reflecting differences in production and loss rates with changes in air-mass origin and/or local emissions. The observed mixing ratios of N_2O_5 are plotted for each night of the campaign in Fig. 2. As described above, NO_3 could not be detected directly using CRD but its mixing ratio was calculated from those of N_2O_5 and NO_2 and the equilibrium constant, K_2. The NO_3 data are generally in good agreement with DOAS measurements considering the differences in location and heights of inlet (CRD) and optical path (LP-DOAS).

As shown in Reactions (R1–R2), the production rates of NO_3 and N_2O_5 are governed by the NO_2 and O_3 mixing ratios. During the DOMINO campaign, night-time mixing ratios of NO_2 were highly variable, fluctuating from local background levels of ∼1 ppbv to more than 15 ppb. The highest levels of NO_2 were associated with air masses that had passed over the Huelva sector, often arriving in plumes with a duration of about 1–2 h. Sub-ppbv levels of NO_2 were usually associated with the Atlantic sector. Apart from infrequent NO spikes presumably from traffic using local roads, night-time levels of NO were low. They were however, occasionally non-zero and on some nights 5–10 pptv of NO was present for a prolonged duration. Given that the lifetime of NO in the presence of >15 ppbv O_3 is only a few minutes, the presence of NO implies a local source. Indeed, with an average night-time wind-speeds of just 2.8 m s^{-1} this implies a source located within about 500 m of the inlet. Possible sources of NO are emissions from the surrounding woodland soil. Apart from occasional plumes from Huelva, non-zero levels of NO were not associated with any single wind-direction which argues against a local, continuous point emission source (i.e. instrument exhaust-line).

Night-time O_3 was strongly anti-correlated with NO_2 and thus also showed significant variability, with typical levels of 15–40 ppbv. Air masses passing over the Huelva and coastal region (and sometimes the open ocean) often contained SO_2, with maximum levels of ∼40 ppbv in plumes originating from the port or Huelva areas. The SO_2 plumes were always associated with high levels of NO_2 with a similar temporal profile, indicating a common process as source. This might have been the result of petrochemical industry activity as flaring at the petrochemical complex in Huelva was frequently visible at night. A further possible source of SO_2 was ship emissions, either at sea or entering the harbour at Huelva. Note that the strait of Gibraltar (∼160 km distant) is one of the world's busiest shipping lanes. SO_2 was not observed above the limit of detection from the continental sector. We note that the presence of both SO_2 and NO_2 in a plume nearly always meant low levels or non-detection of N_2O_5, despite high NO_3 production rates. We discuss this particular aspect of NO_3/N_2O_5 chemistry in more detail later when analysing individual days.

Particles measured at the site displayed number size distributions with mode diameters of between 40 and 80 nm with a generally dominant organic fraction but with a significant sulphate component with short term increases that correlated with SO_2 plumes. The ammonium to sulphate mole ratio was always less than unity during the campaign, indicating that the aerosol was acidic (ratio of 2 = neutral aerosol).

4.1 NO_3 lifetimes

Despite large NO_3 production rates N_2O_5 was only sporadically observed, indicating reactive air-masses and short NO_3 or N_2O_5 lifetimes. More than 50 % of the campaign data revealed NO_3 lifetimes of less than 1 min, with lifetimes longer than 15 min representing only 0.5 % of the measurements. NO_3 lifetimes were found to be strongly dependent on wind direction, with the largest values measured in air masses originating from the Atlantic sector and the shortest lifetimes when air arrived from Huelva, with continental air an intermediate case. This is illustrated in Fig. 3.

During the campaign, NO_3 lifetimes were seen to be reduced at high NO_2 mixing ratios. Frequently, this is taken to be indicative of indirect losses of NO_3 (i.e. N_2O_5 driven, heterogeneous reactions). However, the NO_2 mixing ratio was also correlated with the available surface area, so that separation of the NO_3 losses into direct and indirect reactions (see Eq. 2) is problematic.

Below, we analyse three nights of the campaign in some detail, attempting to identify and quantify the various direct and indirect processes controlling NO_3 lifetimes. Each night represents a different air mass origin, covering each of the Atlantic, Huelva and continental sectors.

4.1.1 6–7 December: clean air from the Atlantic sector

Local wind directions indicated that air masses encountered during the latter part of the night spanning the 6–7 December arrived from the Atlantic sector. Back trajectories (Fig. 1) confirmed that the air had spent at least 3 days over the Atlantic Ocean prior to arriving at the site.

Selected trace gas and aerosol measurements, meteorological data and calculated NO_3 lifetimes are plotted in Fig. 4. After 02:30, O_3 levels were between 25 and 35 ppb, with NO_2 close to 1 ppbv, resulting in comparatively low NO_3 production rates (∼2×10^{-2} ppt s^{-1}). On this night, NO_3 and N_2O_5 measurements started only at 01:45 on the 7th due to instrument tests. N_2O_5 was observed at levels up to ∼50 pptv with NO_3 lifetimes (calculated via Eq. 1) occasionally greater than 30 min. These represent the longest NO_3 lifetimes encountered during the campaign and are consistent with observations of extended NO_3 lifetimes in marine air at low NO_x mixing ratios (Heintz et al., 1996; Carslaw et al.,

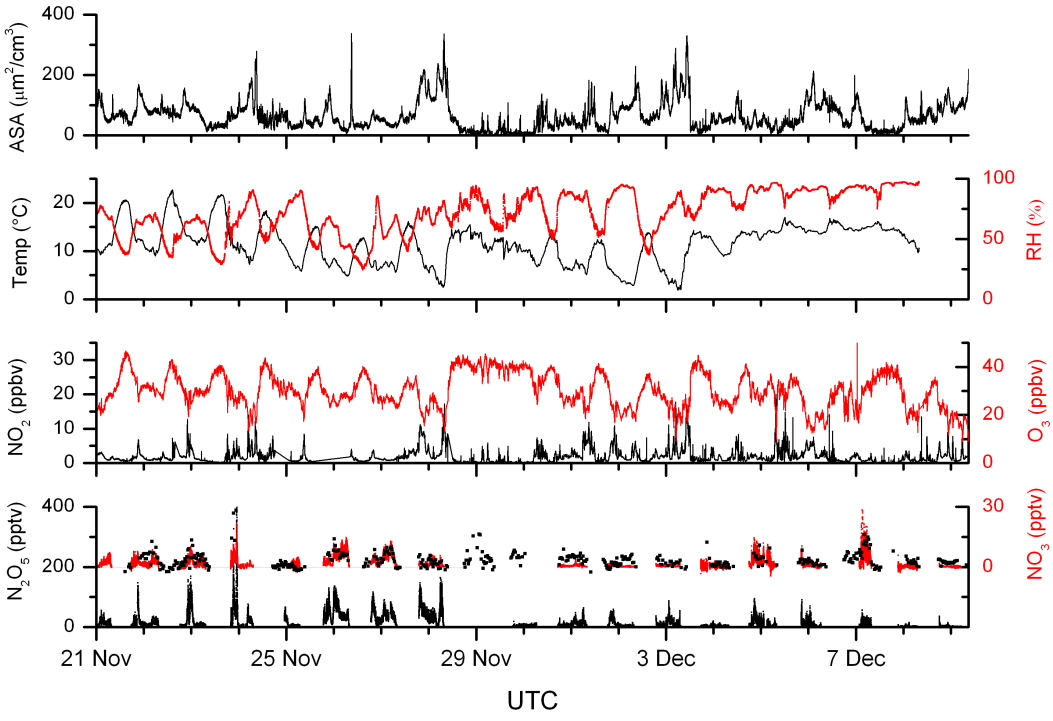

Fig. 2. Campaign overview of measured N_2O_5, NO_2 and O_3 mixing ratios, aerosol surface area (ASA), temperature, relative humidity (RH) and calculated CRD-NO_3 mixing ratios (in red). The black NO_3 datapoints are LP-DOAS measurements. x-axis ticks are at midnight.

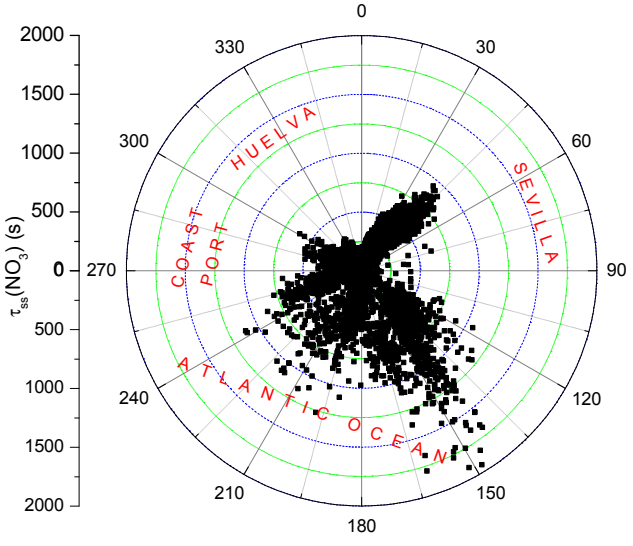

Fig. 3. Wind-direction dependence of NO_3 lifetimes (nighttime only). ∼50 % of the airmasses encountered at night came from the Huelva sector, and were associated with very short NO_3 lifetimes.

1997a, b; Allan et al., 2000). The CRD (calculated) and LP-DOAS derived NO_3 mixing ratios were in good agreement for most of the night. N_2O_5 was, however, not observed before ∼02:30 and its calculated lifetime was less than ∼100 s prior to this time. Similarly, NO_3 lifetimes decreased more or less constantly from 04:30 until dawn. In both cases the short NO_3 lifetime was accompanied by non-zero NO mixing ratios and enhanced NO_2 levels. Prior to 02:30 somewhat reduced O_3 mixing ratios were observed along with elevated levels of SO_2 (2–3 ppbv) and a ∼20 pptv spike in the NO mixing ratio at 02:00, indicating some influence of local emissions. A rough estimate (ignoring dilution) of the age of the NO/NO_2 plume of ∼350 s could be estimated from the enhancement in the NO_2 mixing ratio (∼700 pptv), the NO and O_3 mixing ratios and rate constant for their mutual reaction. The observation of a decrease in a biogenic trace gas (pinene) from 10–20 pptv before 02:30 to 2–3 pptv after 02:30 supports a change in air-mass origin at this time. An increase in NO after 04:30 indicated weak local emissions. The cleanest, maritime air was thus sampled between ∼02:30 and 04:30 on this night.

Three rapid increases in the N_2O_5 mixing ratio (and τ NO_3) at 02:48, 03:20 and 04:06. are apparent in Fig. 4. These features correlate with small increases (less than 1 °C) in the temperature and indicate an influx of air from higher (warmer) layers within the nocturnal inversion, which were less impacted by ground level emissions of e.g. NO or other reactive trace gases. This is a strong indication of large gradients in NO_3 (and N_2O_5) at the site, which were corroborated by DOAS measurements of NO_3 at three different levels (Thieser et al., 2011).

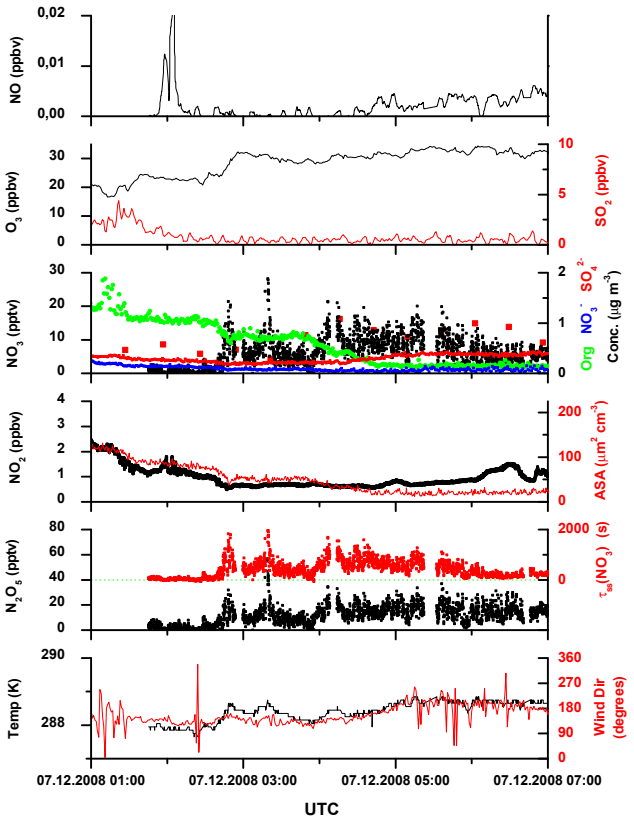

Fig. 4. Overview of measurements on the night 6–7 December (air from the Atlantic sector). ASA = Aerosol surface area. For NO_3, the black datapoints are derived from CRD measurements of N_2O_5, the red squares (at ~30 min intervals) are LP-DOAS measurements.

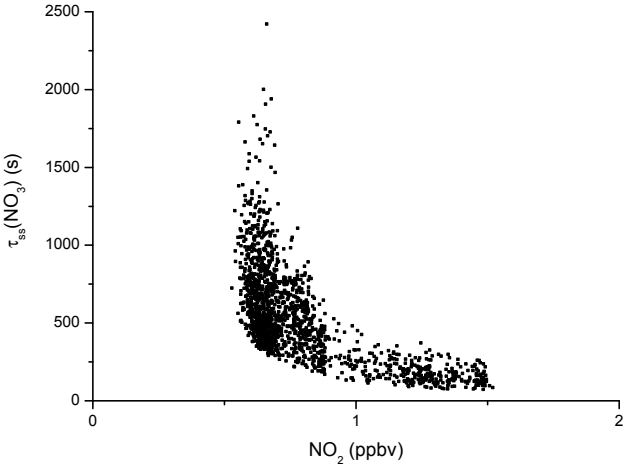

Fig. 5. Dependence of NO_3 lifetime, $\tau_{ss}(NO_3)$, on NO_2 mixing ratios (night 6–7 December). The NO_3 lifetime was calculated using K_2 and measurements of N_2O_5, NO_2 and O_3 (Eq. 1).

In order to understand the factors which limit the NO_3 lifetimes during this night we first estimate the contribution of each constrained loss process for NO_3 and N_2O_5 to see if the summed loss (in the case of N_2O_5 scaled by $K_2[NO_2]$, see Eq. 2) is consistent with observations. Figure 5 reveals that the lifetime of NO_3 was dependent on NO_2 mixing ratios, with the largest lifetimes associated with low NO_2 mixing ratios. Such observations are frequently taken as evidence for an important contribution of N_2O_5 losses to $f_{ss}(NO_3)$ (see Eq. 2) and we consider these first.

Loss of N_2O_5 to aerosols

The uptake coefficient for hydrolysis of N_2O_5 on aqueous, sulphate containing, tropospheric aerosol has been measured using laboratory surrogate aerosol (Mozurkewich and Calvert, 1988; Hu and Abbatt, 1997; Kane et al., 2001; Folkers et al., 2003; Badger et al., 2006; Griffiths and Cox, 2009) and a value of $\gamma \sim 0.04$ at high relative humidity has been recommended (IUPAC, 2010). This is consistent with the largest values of γ derived from calculations using field observations of NO_3 and N_2O_5 (Allan et al., 1999; Aldener et al., 2006; Ambrose et al., 2007; Bertram et al., 2009; Brown et al., 2009). Both laboratory and field work indicate that N_2O_5 uptake coefficients can be significantly lower in the presence of organic components or nitrate, although the presence of chloride can offset the nitrate effect (see e.g. Mentel et al., 1999; Anttila et al., 2006; Bertram and Thornton, 2009; Griffiths et al., 2009; Riemer et al., 2009). Riemer et al. (2009) showed that the uptake coefficient of N_2O_5 on a pure inorganic aerosol depended on the sulphate to nitrate ratio with maximum values of $\gamma(N_2O_5) = 0.02$ on pure sulphate, which reduced to ~0.01 when the sulphate and nitrate masses were equivalent. Bertram et al. (2009) measured N_2O_5 reactivity on ambient aerosol and found for one air sample a maximum value of γ between 0.03 and 0.04 when the ratio of organic-to-sulphate particle mass was ~2.5. This decreased to 0.01 with an organic-to-sulphate ratio of 10. Bertram and Thornton (2009) also describe the particle water molarity dependence of $\gamma(N_2O_5)$ on the uptake of N_2O_5 to NH_4HSO_4 aerosol. Maximum values of $\gamma(N_2O_5) = 0.03$ were found when the H_2O molarity was 20 or greater, but which decreased rapidly below this threshold. Given that the organic mass fraction of the particles was frequently above 50 % before 04:30, lower values of γ than 0.03 will apply irrespective of the nitrate content. Not only the organic mass fraction of the aerosol but also the oxidation state of the condensed organic species influences the rates of uptake of both N_2O_5 and NO_3, either indirectly via the water fraction of the aerosol (N_2O_5) or directly via the number of double bonds available for NO_3 to react with.

During the night 6–7 December the total aerosol surface area was low, consistent with relatively clean maritime air masses, with maximum values of about 90 μm^2 cm^{-3} at the beginning of the NO_3/N_2O_5 measurements and decreasing to ~30 μm^2 cm^{-3} at the end of the night.

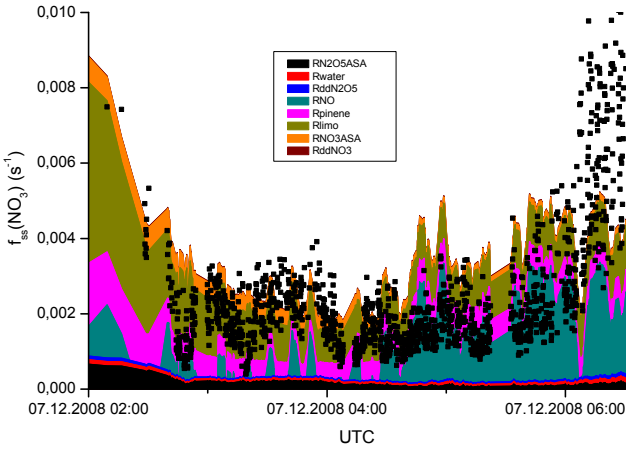

Fig. 6. Apportioned NO_3 loss rates during the night 6th–7th December. The various contributions are: RN_2O_5ASA = uptake of N_2O_5 to aerosol, Rwater = homogeneous hydrolysis of N_2O_5 with water vapour, $RddN_2O_5$ = dry deposition of N_2O_5, RNO = reaction of NO_3 with NO, Rpinene = reaction of NO_3 with α-pinene, Rlimo = reaction of NO_3 with limonene, RNO_3ASA = reaction of NO_3 on aerosol, $RddNO_3$ = dry deposition of NO_3. The solid, black datapoints are measurements of the loss frequency of NO_3.

The organic-to-sulphate ratio was ∼4 until 04:00 when it started decreasing to a value of ∼0.3 to 0.4 clearly indicating a change in air mass to a more marine one at this time. The sulphate to (sulphate + nitrate) ratio was between ∼0.6 and 0.9. The RH was above 90 % all the time so that, late in the night, with high sulphate content and high RH, aqueous aerosol should support a large uptake coefficient, i.e. up to a maximum value of ∼0.04.

The total NO_3 loss rate, $f_{ss}(NO_3)$, calculated using an uptake coefficient of 0.04 for the entire night is displayed in Fig. 6 where various contributors are compared. For most of the night, the low aerosol surface areas meant that N_2O_5 uptake to aerosol (RN_2O_5ASA) accounted for only a few percent to $f_{ss}(NO_3)$ with the exception of periods where the NO_3 lifetime was longest. For example, at 02:00∼10 % of the calculated total loss was due to heterogeneous processing of N_2O_5. When we consider that, especially during the early stages of the measurement, the aerosol had a dominant organic component a lower value than 0.04 for γ would be more realistic, which would further decrease the contribution of N_2O_5 loss. From 04:00 onwards, the contribution of N_2O_5 uptake to $f_{ss}(NO_3)$ diminished as the NO_2 mixing ratio decreased (shifting the NO_3/N_2O_5 equilibrium towards NO_3). At ∼06:00 less than 5 % of the measured loss frequency of NO_3 was due to N_2O_5 losses.

Reaction of N_2O_5 with water vapour

Laboratory experiments (Wahner et al., 1998) have provided evidence for a slow reaction between N_2O_5 and H_2O, which, under certain circumstances, (e.g. low aerosol loading) can contribute to the loss of N_2O_5.

$$N_2O_5 + nH_2O \rightarrow 2HNO_3 + (n-1)H_2O \quad \text{(R4)}$$

The reaction was found to proceed with terms both linear and quadratic in $[H_2O]$ so that the loss rate coefficient (k_{H_2O}) is described by $k_{H_2O} = 2.5 \times 10^{-22}$ $[H_2O] + 1.8 \times 10^{-39}$ $[H_2O]^2$ s^{-1}. Measurements of long N_2O_5 lifetimes at high relatively humidity (Brown et al., 2009) strongly suggest that the true value may be a factor 10 lower. We therefore assess the impact of this reaction on NO_3 lifetimes using $0.1 \times k_{H_2O}$. This is displayed as Rwater of Fig. 6. At rates of $<1 \times 10^{-4}$, reaction with H_2O has an insignificant impact on the overall loss rate of N_2O_5 (or NO_3) throughout the entire night.

Dry deposition of N_2O_5

Assuming neutral stratification and zero surface resistance (Geyer et al., 2001a) calculated an upper limit to the N_2O_5 loss frequency due to dry deposition within a 100 m high nocturnal boundary layer as 0.3×10^{-4} s^{-1}. When multiplied by $K_2[NO_2]$, this results in a loss rate constant for NO_3 of $<1 \times 10^{-4}$ s^{-1}, contributing insignificantly to the NO_3 lifetime (Rdd N_2O_5 Fig. 6). Assuming a factor two lower (or higher) boundary layer would not alter this conclusion.

Gas-phase reactions of NO_3

Known reaction partners for NO_3, which were constrained by measurements were NO, α-pinene, isoprene and HCHO. The reactions of NO_3 with both NO and α-pinene have large rate coefficients ($k_5 = 2.6 \times 10^{-11}$, $k_6 = 6.2 \times 10^{-12}$ cm^3 $molecule^{-1}$ s^{-1}) whereas HCHO reacts much more slowly ($k_9 = 5.6 \times 10^{-16}$ cm^3 $molecule^{-1}$ s^{-1}). Isoprene is an intermediate case with $k_7 = 7 \times 10^{-13}$ cm^3 $molecule^{-1}$ s^{-1} (Atkinson et al., 2004, 2006). At mixing ratios of less than 1 ppbv on this night HCHO did not contribute significantly to NO_3 removal and is not further considered. Likewise, isoprene mixing ratios on this night were less than those of α-pinene and limonene and as isoprene reacts a factor ∼10 slower than α-pinene or limonene with NO_3, we do not need to consider Reaction (R7).

$$NO_3 + NO \rightarrow 2NO_2 \quad \text{(R5)}$$

$$NO_3 + \alpha - \text{pinene} \rightarrow \text{products} \quad \text{(R6)}$$

$$NO_3 + \text{isoprene} \rightarrow \text{products} \quad \text{(R7)}$$

$$NO_3 + \text{limonene} \rightarrow \text{products} \quad \text{(R8)}$$

$$NO_3 + HCHO \rightarrow HNO_3 + HCO \quad \text{(R9)}$$

The calculated, steady state, turnover loss rates of NO_3 for reaction with NO (RNO), α-pinene (Rpinene) and limonene (Rlimo) are illustrated in Fig. 6. Loss of NO_3 due to reaction

with α-pinene and limonene was slow, reflecting the low concentrations and emission rates of biogenic trace gases during late autumn at this site (Song et al., 2011), but still significant in the early part of the night, where its contribution easily exceeds that of heterogeneous losses. The reaction with NO is unimportant until ~04:00 but thereafter becomes the dominant NO_3 sink for the rest of the night and even at mixing ratios of just 5 pptv can account for the entire observed NO_3 loss until ~06:00. After 06:00, the reaction of NO accounts for ~30 % of the observed NO_3 loss rate. Note that fine structure on the NO_3 loss rate due to Reaction (R5) (RNO) is due to noise as the measurements were made close to the NO detection limit.

Loss of NO_3 to aerosols and via dry deposition

Laboratory experiments have characterised the efficiency of uptake of NO_3 to various environmental surfaces. Whereas the low solubility of NO_3 in water leads to low uptake coefficients ($\gamma_{NO_3} \leq 10^{-3}$) for interaction with aqueous droplets (Rudich et al., 1996), large values ($\gamma_{NO_3} \sim 0.1$) have been found for uptake to low volatility, unsaturated organic liquids (Moise et al., 2002; Gross and Bertram, 2009; Gross et al., 2009), such as those present in secondary organic aerosol. Uptake of NO_3 to urban aerosol (Tang et al., 2010) or organic aerosols (Gross et al., 2009) has been found to be orders of magnitude more efficient than N_2O_5 uptake to the same aerosol type. For the purpose of assessing the contribution of heterogeneous NO_3 loss to aerosol we have used a value of $\gamma = 0.1$, which most probably represents an upper limit to the true value. Despite the use of this large value, the loss of NO_3 to aerosol is not significant (RNO_3ASA in Fig. 6) but nonetheless exceeds N_2O_5 loss rates via uptake to aerosol when NO_2 is low (i.e. when the NO_3/N_2O_5 equilibrium is not strongly partitioned towards N_2O_5) as seen between 02:00 and 04:00. As for N_2O_5, dry deposition ($RddNO_3$) is insignificant if a loss rate of 0.3×10^{-4} s^{-1} is adopted (Geyer et al., 2001a).

Summary

Some of the cleanest air-masses encountered at night in the campaign reached the measurement site on the night of 6–7 December and NO_3 lifetimes were correspondingly long. A large fraction (and sometimes all) of the NO_3 reactivity was accounted for with measured parameters as summarised in Fig. 6.

Although the results suggest that the aerosol loss of N_2O_5 contributed up to 20 % to NO_3 losses early in the night, recall that the γ used was most likely too high for aerosol with a dominant organic fraction and thus may be considered an upper limit. Missing reactivity (i.e. measured NO_3 lifetimes were shorter than calculated based on measured parameters) was apparent between circa 03:00 and 04:00 and also after 06:00. The deviation between measured and calculated NO_3 lifetimes is similar in direction and magnitude to that observed previously in marine air masses (Sommariva et al., 2007).

Considering that this air mass had spent several days over the ocean, CH_3SCH_3 (not measured) is a likely contributor to NO_3 reactivity. Strong evidence for CH_3SCH_3 in this air mass could be found in AMS measurements of significant methane-sulphonic acid concentrations on the morning of 7 December. Given a rate constant for reaction between NO_3 and CH_3SCH_3 of 1.1×10^{-12} cm^3 molecule^{-1} s^{-1} (Atkinson et al., 2004) the missing reactivity observed at ~06:00 (about 0.005 s^{-1}) would be provided by ~200 pptv of CH_3SCH_3.

As already mentioned, the plot of NO_3 lifetime versus NO_2 (Fig. 5) could be interpreted to indicate that indirect loss of NO_3 (i.e. via N_2O_5 removal) is an important contributor to NO_3 lifetimes. The discussion above indicates however, that the indirect losses are inefficient and a weak correlation between NO_2 and NO explains the dependence of NO_3 lifetimes on NO_2. At high NO_2 mixing ratios (e.g. 1–1.5 ppb) the calculated lifetimes are larger than measured. These data points were taken at the end of the night (after 06:00) and Fig. 6 also indicates missing reactivity during this period. In the absence of a significant change in wind direction, the plume like NO_2 increases (about 0.5 ppb) during this part of the night may indicate local ship emissions and an increase in reactivity towards NO_3 due to other trace gases co-emitted.

As a significant fraction of the NO_3 reactivity is accounted for by measured NO (which must have a local source) the use of a steady-state analysis for the later part of this night is not entirely appropriate.

Low nighttime concentrations of NO have previously been reported to limit NO_3 lifetimes in a relatively clean coastal environment, which may be impacted by local NO emissions, e.g. from soil (Sommariva et al., 2007).

4.1.2 23–24 November: mixed air from the continental and Huelva sectors

Measurements of N_2O_5 on this evening started at 20:00 UTC, about 2.5 h after sunset. The complete dataset, with meteorological information and other trace gas measurements is displayed in Fig. 7. Until midnight, the wind was mainly from the continental sector (close to 360 degrees) whereas after midnight it came mainly from the Huelva/Port sectors. Following a warm, cloud-free day, the night of the 23–24 November was characterised by low wind speeds and a strong temperature inversion (temperature at 50 m was ~7 °C higher than at inlet height), implying a highly stratified nocturnal boundary layer. Back trajectories (Fig. 1) suggest that the air had travelled over the Atlantic before spending 1 day over central Spain with the last 6–12 h within the boundary layer.

NO_2 levels showed large variability during the night with mixing ratios between 1 and 13 ppbv, whereas NO was

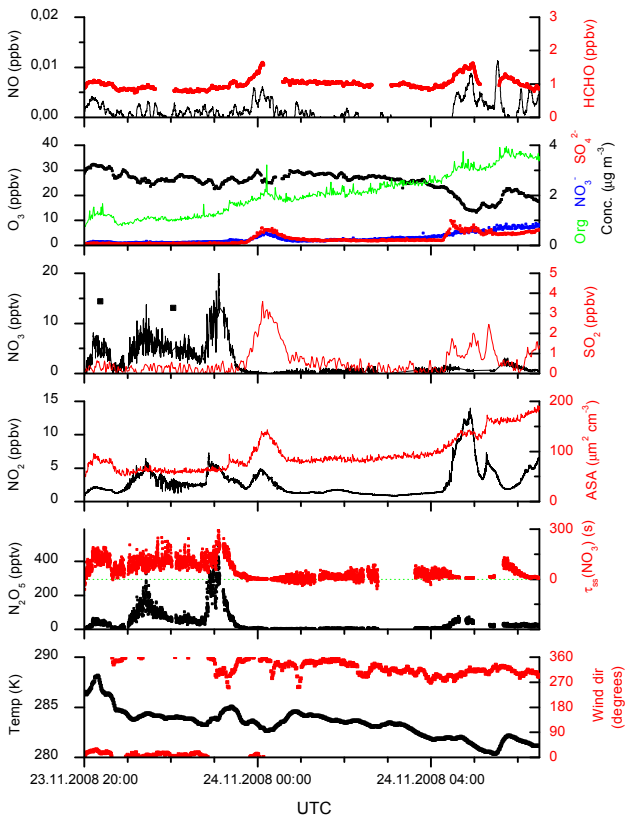

Fig. 7. Overview of measurements on the night 23rd–24th in which wind direction swung from the continental to Huelva sector. Only limited LP-DOAS measurements (solid black symbols) were available from the lowest optical path on this night.

always close to zero (<2 pptv) until about 04:30 when a few pptv were observed. Some plume like NO_2 features were accompanied by plumes of similar duration in SO_2 (up to ~3 ppbv), HCHO (up to ~1.5 ppbv) and increases in the overall aerosol surface area, implying common, likely combustion related sources. This is especially apparent in the plumes at midnight and 05:00. For each of the NO_2 plumes at ~20:00, 21:30 and 23:00 there is a significant increase in the N_2O_5 mixing ratio, caused by an increase in the NO_3 production rate. In contrast, N_2O_5 remains close to the detection limit for the entire NO_2 plume at midnight and reaches only low mixing ratios during the larger plumes at 05:00 and 06:30. Note that the NO_2 plume at ~23:00 (when SO_2 was close to zero) was accompanied by a positive gradient in the temperature, whereas the NO_2/SO_2 plume at midnight was accompanied by a negative temperature gradient. Similarly the NO_2/SO_2 plumes after 04:00 were accompanied by drops in temperature. The NO_2/SO_2 plumes were also accompanied by an increase in the aerosol surface area, caused by an increase in mainly the sulphate and nitrate content, but also the organic fraction of the aerosol.

Prior to midnight, NO_2 mixing ratios between ~1 and 6 ppbv and ozone levels of >25 ppbv resulted in large NO_3 production rates (up to ~0.12 pt s^{-1}) and the highest N_2O_5 mixing ratios in the entire campaign (~500 ppt) were measured. The high levels of NO_2 and moderately cold temperatures (283 K) meant that N_2O_5 was usually in greater than tenfold excess of the calculated NO_3 mixing ratio, and up to a factor of 50 greater at the peak of the NO_2 plumes. Prior to midnight, $\tau_{ss}(NO_3)$ was fairly constant at about 75–150 s but was essentially zero for the period between midnight and 01:00 during the SO_2 plume. Log-book entries report significant levels of malodorous gases at the site. The dependence of the NO_3 lifetime on NO_2 and SO_2 mixing ratios and aerosol surface area (ASA) is summarised in Fig. 8. The shortest NO_3 lifetimes are clearly associated with large NO_2 concentrations (upper panel), likewise SO_2 mixing ratios above 1 ppbv are always associated with very short NO_3 lifetimes and there is also weak anti-correlation with aerosol surface area. The observed NO_2 and aerosol surface area dependencies would appear to indicate that heterogeneous loss of N_2O_5 is important. Similar to the treatment above for the Atlantic sector we therefore assess (via Eq. 2) gas-phase and heterogeneous loss mechanisms for NO_3 and N_2O_5 which were constrained by measurements and also identify potential (unmeasured) reactive trace gases.

Heterogeneous loss of NO_3 and N_2O_5

Compared to 7 December, the surface area available for interaction of aerosol with N_2O_5 or NO_3 was significantly larger on this night (factor of 2–3). The high levels of NO_2 observed result in large N_2O_5/NO_3 ratios, so that the heterogeneous losses would be expected to be more important for N_2O_5 than for NO_3. For this night the aerosol contained a very high organic component (up to 75 % of the aerosol mass) with organic/sulphate ratios as high as 15 early in the night and never decreasing below about 3. The sulphate/(sulphate + nitrate) ratio was also quite low (0.3–0.7). As discussed above, $\gamma(N_2O_5)$ on such particles would be expected to be less than 0.04. The uptake coefficient for NO_3 is poorly defined but potentially a factor of 10 larger (Tang et al., 2010). An absolute upper limit to the sum of direct and indirect NO_3 loss rates via heterogeneous uptake to aerosol was thus calculated using uptake coefficients of 0.04 for N_2O_5 and 0.5 for NO_3, the later representing diffusion limited uptake. This provides an estimate of the maximum contribution of heterogeneous reactions on aerosols to the NO_3 lifetime.

Figure 9 provides an overview of the relative importance of the constrained, direct and indirect loss processes for NO_3 on this night. Even though the uptake coefficients employed were upper limits, the calculated loss of N_2O_5 (RN_2O_5ASA) and NO_3 (RNO_3ASA) to aerosols does not account entirely for the observed NO_3 loss frequency (black dots) before ~23:30 on the 23rd. Despite the much larger uptake coefficient used for NO_3, its contribution to the total heterogeneous loss was similar to that of N_2O_5 as the NO_3-N_2O_5

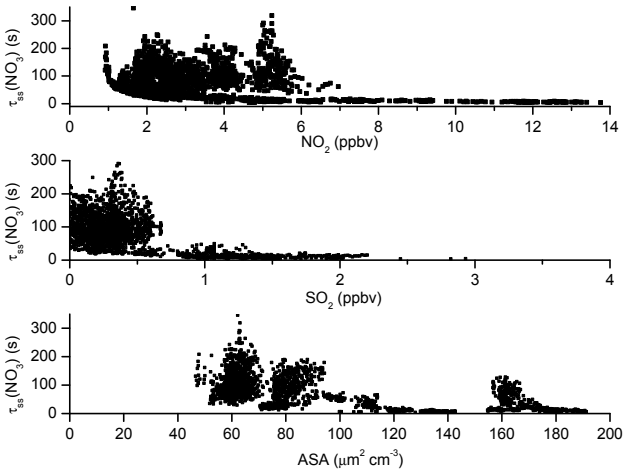

Fig. 8. 23–24 November: dependence of $\tau_{ss}(NO_3)$ on NO_2 and SO_2 mixing ratios and the aerosol surface area (ASA). $\tau_{ss}(NO_3)$ was calculated using measurements of N_2O_5, NO_2 and O_3 (Eq. 1).

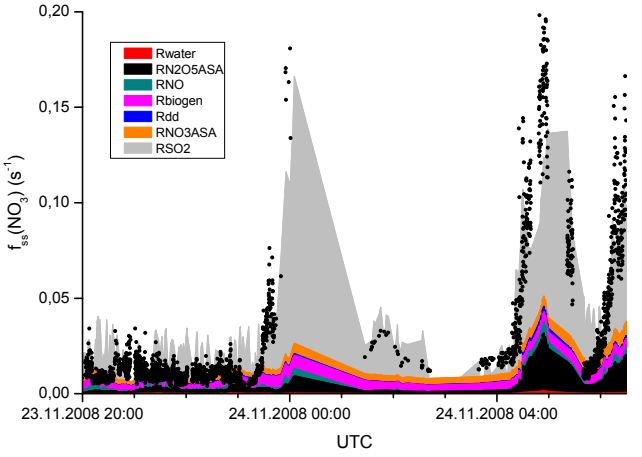

Fig. 9. Apportioned NO_3 loss rates on the night 23–24 November. The various contributions are: Rwater = homogeneous hydrolysis of N_2O_5 with water vapour, RN_2O_5ASA = uptake of N_2O_5 to aerosol, RNO = reaction of NO_3 with NO, Rbiogen = reaction of NO_3 with isoprene, limonene and α-pinene, Rdd = summed dry deposition of N_2O_5 and NO_3, RNO_3ASA = reaction of NO_3 on aerosol, RSO_2 is the missing reactivity which has been scaled to correlate with SO_2 mixing ratios. The black dots datapoints are the calculated loss frequency of NO_3 .

partitioning was shifted towards N_2O_5 on this night with high NO_2 mixing ratios.

During the first SO_2/NO_2 plume (centred at midnight) the NO_3 lifetime was drastically shortened and heterogeneous processes contribute an upper limit of ∼10 % to the overall measured loss frequency of NO_3 ($RN_2O_5ASA + RNO_3ASA$). Similarly, the summed effect of dry deposition of NO_3 and N_2O_5 (using the dry deposition rates listed above) can be disregarded as a major loss of either NO_3 or N_2O_5 (Rdd).

Gas-Phase reactions of NO_3 and N_2O_5

Similar to 7 December, the homogeneous hydrolysis of N_2O_5 is not an important loss process in this air mass, contributing less than 1 % to the NO_3 reactivity (Rwater of Fig. 9). Close to zero levels of NO during most of this night also rule out a significant impact (RNO). The sum of the direct NO_3 loss rates due to BVOC (the sum of α-pinene, limonene and isoprene, Rbiogen) contributes significantly to NO_3 loss before 23:00, but only a few percent during the SO_2 plumes. Further measured trace gases which can react with NO_3 are HCHO and aromatics. At a mixing ratio of close to 1 ppbv and a rate coefficient close to 5×10^{-16} cm^3 $molecule^{-1}$ s^{-1} (Atkinson et al., 2006) HCHO can contribute a negligible 1×10^{-5} s^{-1} to the overall NO_3 loss rate. Similarly, with respective room temperature rate coefficients of $<3 \times 10^{-17}$, 7×10^{-17}, $\sim 4 \times 10^{-16}$ and $<6 \times 10^{-16}$ cm^3 $molecule^{-1}$ s^{-1} (Atkinson and Arey, 2003), benzene (∼80 pptv), toluene (∼100 pptv), xylenes (sum of *p*, *m* and *o*-xylene was ∼20 pptv) and ehylbenzene (8 pptv) all react too slowly with NO_3 to contribute significantly.

Under certain circumstances, RO_2 (formed e.g. from NO_3 initiated oxidation of CH_3SCH_3 or ozonolysis of BVOC) has been shown to contribute to NO_3 loss (Sommariva et al., 2009). On this night, RO_2 mixing ratios of up to 80 pptv were observed between ∼midnight and 04:00 (Andrés-Hernández et al., 2011). In the absence of speciated RO_2 measurements we calculate the loss rate of NO_3 due to reaction with RO_2 assuming a rate coefficient of 2.3×10^{-12} cm^3 $molecule^{-1}$ s^{-1} taken from evaluated kinetic data (Atkinson et al., 2006). This results in NO_3 loss rates of $\sim 5 \times 10^{-3}$ s^{-1}, which again is only a small fraction of the total loss rate (∼4 % at midnight).

Clearly, the sum of constrained indirect and direct losses of NO_3 do not explain the short lifetimes observed during the SO_2 plumes. As heterogeneous processing cannot be enhanced in rate beyond that calculated using measured aerosol surface areas and upper limits for $\gamma(NO_3)$ and $\gamma(N_2O_5)$ we turn to potential gas-phase reactions, that were not constrained by measurements at the site.

Unknown or undetermined reactions/loss processes

The aerosol surface area and trace gases which were measured provided only a fraction of the observed reactivity after midnight on the 23rd–24th. A clue to the missing reactivity may be provided by the very short NO_3 lifetimes (or absence of N_2O_5) when SO_2 was present at levels above ∼1 ppbv (Figs. 7 and 8).

Whilst SO_2 itself does not react with NO_3, it may be co-emitted or co-located with emissions of more reactive traces gases. Two scenarios are considered below in which reduced

sulphur species or unsaturated VOCs are responsible for efficient NO_3 loss during periods of enhanced SO_2 on this night.

A log-book entry describes strongly malodorous air at the measurement site on this (and several other) nights. Malodorous, reduced sulphur compounds (RSC) are often associated with oil refining, pulp/paper mill and waste treatment activities (Nunes et al., 2005; Pal et al., 2009; Toda et al., 2010) and we note that not only a huge oil-refinery complex but also Spain's largest pulp/paper mill is located in Huelva.

RSC with high reactivity to NO_3 are CH_3SCH_3 (DMS), CH_3SSCH_3 (DMDS) and CH_3SH. NO_3 lifetimes are known to be strongly influenced by DMS emissions in marine air masses (Allan et al., 2000; Aldener et al., 2006; Sommariva et al., 2009) but a large contribution to NO_3 loss in urban air has also been reported (Shon and Kim, 2006). The oxidation of RSC by NO_3 results in the formation of SO_2, HCHO and RO_2 (Jensen et al., 1992) with (modelled) RO_2 levels often exceeding those observed during daylight (Sommariva et al., 2009). The rate coefficients for reaction of DMS, DMDS and CH_3SH with NO_3 are all close to 1×10^{-12} cm^3 molecule^{-1} s^{-1}, so that a total mixing ratio of these RSC of 4 ppbv would provide an equivalent reactivity of 0.1 s^{-1}. Whilst no measurements of RSC were available to support their potential role, we note that ppbv mixing ratios are not unrealistic as RSC emitted into a shallow, highly stratified boundary layer at night have no gas-phase loss mechanisms apart from reaction with NO_3. Human odour thresholds for H_2S, CH_3SH, CH_3SCH_3 and CH_3SSCH_3 are also in the ppbv regime (Kim et al., 2007; Pal et al., 2009). In order to capture the NO_3 lifetime dependence on SO_2, a reactive term, considering the presence of a trace gas at a constant fraction of the SO_2 mixing ratio and reacting with NO_3 with a rate constant of 1×10^{-12} cm^3 molecule^{-1} s^{-1} (i.e. like RSC) was added to Eq. (2). The result is the grey area (RSO2) of Fig. 9. The RSC to SO_2 ratio was adjusted (to ∼2) to approximately capture the large NO_3 loss rates at midnight, bringing the measured and modelled steady state lifetime in rough agreement.

The co-incidental increases in nighttime aerosol surface area and the sulphate component of the aerosol is difficult to account for in the RSC scenario unless a sufficient rate of oxidation of SO_2 (i.e. by reaction with OH) is available. Nighttime OH could conceivably be generated by reactions of RO_2 with NO_3 (Platt et al., 1990; Geyer et al., 2003). The increase in particle sulphate at the maximum of the 3 ppbv SO_2 plume was ∼0.5 µg m^{-3}, which would require oxidation via reaction with OH of 100 pptv of SO_2 and efficient transfer of the H_2SO_4 product to the particle phase. Assuming a total reaction time of 4 h (maximum transport time from Huelva), this would still require a constant nighttime OH concentration en route of $\sim 2 \times 10^6$ molecule cm^{-3}.

Interactions between NO_x and reduced sulphur thus provide an interesting but highly speculative explanation for some of the observations on this and other campaign nights, including short NO_3 lifetimes, high RO_2 levels and formation of HCHO and SO_2, though we note that plume like increases in SO_2 were not always accompanied by increases in HCHO as illustrated for this night in Fig. 7.

In a second scenario, we consider the coincident arrival of the SO_2, NO_2 and HCHO plumes to be due to their formation in a common combustion source, either related to shipping or oil-refinery activity. During this night the wind direction swept slowly from the continental sector to the Huelva sector with the plumes in NO_2 reflecting emissions from various point sources in the coastal-Huelva region. The short lifetimes of NO_3 after midnight reflect highly reactive air masses from Huelva, but not necessarily due to RSC. Hydrocarbon emissions related to the petrochemical industry, including unsaturated VOC such as 1,3-butadiene (Roberts et al., 2003) which are reactive towards NO_3 could then be responsible for the short NO_3 lifetimes. In this scenario, the source of the peroxy radicals observed on this night would be reaction of unsaturated hydrocarbons with either NO_3 or O_3. In this context note that NO_3 reacts at least a factor 10 more slowly with unsaturated, petrochemical-related hydrocarbons (e.g. the rate coefficient for NO_3 with 1,3-butadiene is 1.0×10^{-13} cm^3 molecule^{-1} s^{-1}) than with RSC so that mixing ratios of several tens of ppbv of the alkene would be necessary to explain the short NO_3 lifetimes. In summary, air from the Huelva sector and the port/coastal region close to Huelva was highly reactive towards NO_3 resulting in very short lifetimes which were controlled by gas-phase reactions and a diminished role for heterogeneous processes (either for NO_3 or N_2O_5). Whilst RSC and unsaturated VOC were proposed as potential reaction partners for NO_3 they were not constrained by measurements and for extended periods of the night (especially when SO_2 was observable) much of the reactivity is not accounted for.

4.1.3 26–27 November: air from the continental sector

On the night of 26–27 November, local wind directions indicated air masses originating from continental Spain which avoided large local cities and industrial centres such as Huelva or Sevilla. Back trajectories suggested that the air had spent the last two days over central Spain and northern France before reaching the site, gradually descending from ∼3500 m to ground level over this period with only the last 4–6 h spent at altitudes of less than 500 m. Local wind speeds during the night were between 2.5 and 5 m s^{-1}.

On this night, NO_2 levels were generally under 2 ppbv except for a plume-like increase to ∼4 ppbv at ∼20:00 on the evening of the 26th (Fig. 10). As was frequently observed for the continental sector, NO_2 was correlated with black carbon but not with SO_2, indicating that emission by road traffic was the most likely source. NO was close to the detection limit (2 ppt) during the whole night, except for some spikes due to very local (likely vehicular) emissions. The constancy of the NO mixing ratio through the night strongly suggests that the true value is zero and the 2 pptv is a residual from

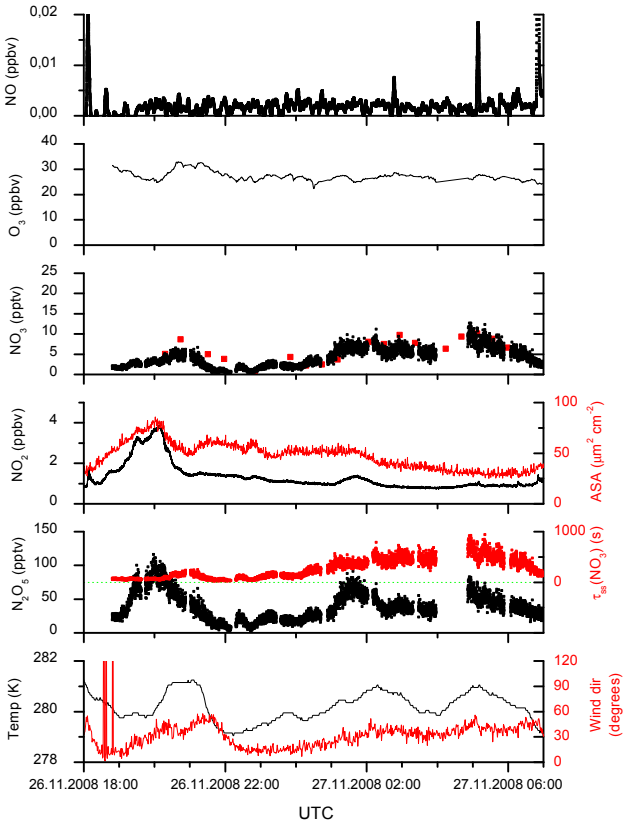

Fig. 10. Overview of measurements on the night of 26–27 November (air from the continental sector). For NO_3, the black dataponts are CRD measurements, the red squares (~30 min resolution) are DOAS measurements.

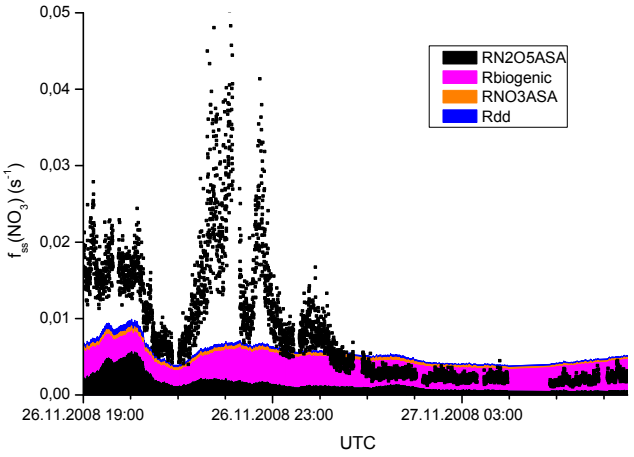

Fig. 11. Apportioned NO_3 loss rates on the night 26th–27th of November. The various contributions are: RN_2O_5ASA = uptake of N_2O_5 to aerosol (using $\gamma = 0.04$), Rbiogenic = reaction of NO_3 with isoprene, limonene and α-pinene, RNO_3ASA = reaction of NO_3 on aerosol (using $\gamma = 0.1$), Rdd = summed dry deposition of N_2O_5 and NO_3. The black datapoints are measurements of loss frequency of NO_3.

zero correction. O_3 levels were constant at ~25–30 ppbv. Levels of biogenic hydrocarbons (isoprene, pinene) were low (~10 ppt) as on other nights of the campaign. Mixing ratios of aromatics were similar to the 23rd (less than 100 pptv). Aerosol surface areas were between 25 and 80 $\mu m^2\ cm^{-3}$ and were correlated with NO_2. The aerosol was acidic ($NH_4^+/SO_4^{2-} = 0.6$) with a dominant organic fraction (the organic to sulphate ratio was ~4 until 04:00 when it slowly decreased to 2).

N_2O_5 could be measured above the detection limit at almost all times during this night, with maximum mixing ratios of ~100 pptv and steady-state NO_3-lifetimes up to 900 s. Intermediate to those observed for the Huelva and Atlantic sectors. The CRD and DOAS-derived NO_3 mixing ratios were in good agreement, especially after midnight. The observations are summarised in Fig. 10.

As in the discussion of the previous case studies, direct and indirect losses of NO_3 were assessed based on measured aerosol surface areas and trace gases. For this purpose, NO mixing ratios were assumed to be zero. The calculations are summarised in Fig. 11. Between midnight and 07:00, the presence of α-pinene and limonene at mixing ratios of 5–10 pptv results in loss rates of $\sim 4 \times 10^{-3}\ s^{-1}$. The calculated NO_3 loss rate in this period thus exceeds that measured suggesting that reactivity is entirely accounted for by reasonably well constrained gas-phase reactions. This allows us to estimate upper bounds for the rates of all other loss mechanisms, including uptake to aerosol on this night. The rate of direct loss of NO_3 to the organic component of the aerosol is of major uncertainty as the nature of the organic fraction (and thus availability of e.g. double bonds with which NO_3 can react) is unknown. A value of γ $NO_3 = 0.1$ contributes only insignificantly to the NO_3 lifetime whereas a value of 0.5 (diffusion limited uptake) would increase the discrepancy between observed and calculated lifetimes. A similar effect would be obtained by use of a large value (e.g. 0.1) for $\gamma(N_2O_5)$. On this night, the organic to sulphate ratio was ~2–4 and the sulphate to (sulphate + nitrate) ratio was fairly constant at 0.6, implying a more likely value of γ (N_2O_5) of ~0.01 (Riemer et al., 2009), which is also consistent with our observations. In the first half of the night (up to ~midnight) NO_3 lifetimes were much shorter and highly variable, with loss rates up to $0.05\ s^{-1}$ (lifetimes of just 200 s). We can rule out that this increase in the NO_3 loss frequency is due to a change in reactivity of the aerosol to either N_2O_5 or NO_3. Neither the aerosol composition (i.e. organic, nitrate and sulphate fractions and acidity) nor the relative humidity changed significantly during the night so a large change in γ (factor 10) is not anticipated. Also, the large variability in the loss frequency is not mirrored by changes in aerosol surface area, but is most likely associated with fluctuations in rates of vertical mixing within a highly stratified nocturnal boundary layer, with longer lived NO_3 present in higher

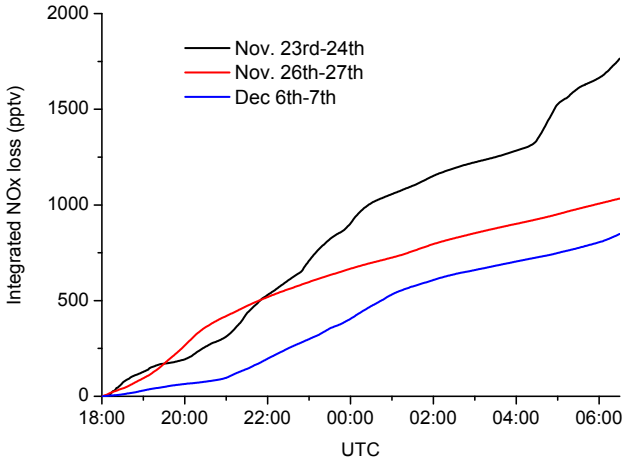

Fig. 12. Integrated loss of NO_x on three campaign nights with air from the Huelva sector (black line), the continental sector (red line) and the Atlantic sector (blue line). Mean NO_2 concentrations on these nights (18:00 til 06:30) were 2.7, 1.3 and 1.2 ppbv, for the 23–24th, 26–27th and 6–17th, respectively.

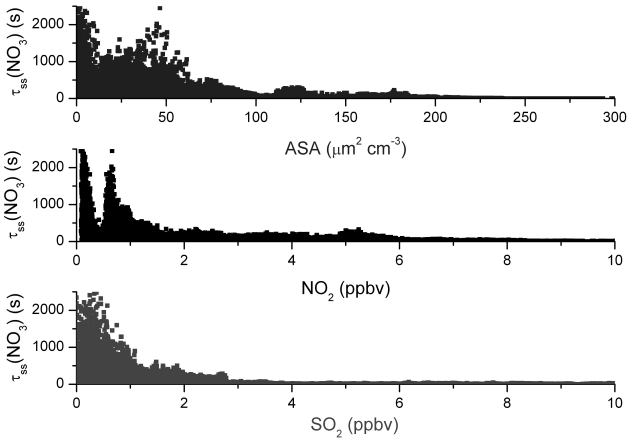

Fig. 13. Relationship between NO_3 lifetimes, $\tau_{ss}(NO_3)$ and the mixing ratios of NO_2, SO_2 and aerosol surface area (ASA) during the entire campaign.

layers. Inspection of the temperature and N_2O_5 trends during this night reveals significant correlation, with higher temperatures (i.e. air from higher altitudes) bringing more NO_3. Measurements of a strong vertical gradient in N_2O_5 on this night (Thieser et al., 2011) confirm this interpretation.

4.2 Nocturnal loss of NO_x and VOCs

During DOMINO, the efficiency of nocturnal loss of NO_x to particulate phase or to long-lived reservoir species (e.g. HNO_3) which may undergo deposition, will depend both on the absolute and relative rates of processing of NO_3 (in gas-phase reactions) and N_2O_5 (in heterogeneous reactions). If direct loss processes of NO_3 are slow and N_2O_5 uptake to particles is inefficient, the NO_3-N_2O_5 equilibrium-pair represents only a temporary NO_x reservoir. N_2O_5 or NO_3 formed in the night will release NO_x at sunrise as NO_3 lifetimes are shortened by photolysis (to form both NO and NO_2) and reaction with NO (to form NO_2). N_2O_5 decomposes thermally to NO_2 and NO_3, so that NO_x is recovered and available for O_3 production. In the present campaign, nighttime lifetimes of NO_3 were generally so short that efficient irreversible loss of NO_x occurred. NO_3 lifetimes of just a few minutes imply that the rate of loss of boundary layer NO_x is approximately equal to the rate of NO_3 formation i.e.

$$L_{NO_x} \approx n \cdot k_1[NO_2][O_3] \quad (5)$$

where the factor n is 1 if NO_3 is lost only directly (e.g. by reaction with VOC) and is 2 if NO_3 is lost indirectly only via N_2O_5 formation and reaction as two NO_2 are required to make each N_2O_5 molecule. For the present campaign we have shown that, when produced at high rates, NO_3 is lost predominantly by direct routes, so that n should be close to 1. Figure 12 displays the integrated NO_x losses via reaction of NO_2 with O_3 for the three case studies outlined above. These calculations indicate that over the course of a 12 h night, 0.8, 1.0 and 1.8 ppbv of NO_x were removed from the boundary layer on the 23–24th, 26–27th and 6–7th, respectively. This is equivalent to ∼70 % of NO_2 as mean mixing ratios were 1.2, 2.7 and 1.3 ppbv on these nights. The average loss rates were in the range 1.9–4.2 $\times 10^{-5}$ ppbv of NO_2 per second. Assuming that NO_3 is lost entirely by reaction with VOC (and not reaction with NO or by NO_3 or N_2O_5 uptake to aerosol), this is also the loss rate of VOC over the same period. For comparison, a 12 h, daytime loss of NO_2 via reaction with OH of 2×10^{-5} s^{-1} would be obtained for average OH and NO_2 mixing ratios of 0.04 and 2000 ppt, respectively, though the greater daytime boundary layer depth would favour the OH mechanism.

5 Summary and conclusions

Measurements of N_2O_5 and steady-state calculations of NO_3 lifetimes during the DOMINO campaign revealed stark differences according to the type of air mass encountered. The longest lifetimes (∼30 min) of NO_3 were encountered in air masses arriving from the Atlantic sector. Air from the Huelva urban (petrochemical and industrial) sector had high production rates of NO_3, but frequently concentrations close to the detection limit and lifetimes of only a few seconds. The high reactivity could only be partially accounted for by measured trace gases and aerosol surface areas. Lifetimes of NO_3 were always very short when SO_2 was observed at the site, either due to reactions of NO_3 with RSC or due to common or co-located emissions (e.g. combustion) sources of other reactive trace gases. The relationship between the NO_3 lifetime, SO_2, NO_2 and ASA over the course of the entire campaign

is illustrated in Fig. 13. Clearly, polluted air masses (NO_2 or $SO_2 > 2$ ppbv) do not support long NO_3 lifetimes.

NO_3 in air from the continental sector had lifetimes which were similar to other forested areas (e.g. Crowley et al., 2010), but which were occasionally significantly shortened, presumably due to the impact of anthropogenic emissions. In general these results show that NO_3 (or N_2O_5) mixing ratios in air masses from urban and industrial centres were controlled by gas-phase reactions of NO_3 and cannot be accurately estimated from production terms (e.g. NO_2 and O_3 mixing ratios) and measured BVOC and aerosol. However, the combination of high NO_3 production rates and short lifetimes frequently observed during the campaign implies large nocturnal processing rates for the VOCs mainly responsible for NO_3 loss, and thus a high production rate of organic peroxy radicals and secondary oxidation products, such as carbonyl compounds and organic nitrates/nitric acid.

Acknowledgements. We are indebted to the National Institute for Aerospace Technology (INTA) for hosting the campaign and to Monica Martinez (Max-Planck-Institut) for campaign organisation and management. We thank Pablo Hidalgo for information related to industrial activity in the Huelva area. We thank DuPont for providing us with the FEP dispersion.

The service charges for this open access publication have been covered by the Max Planck Society.

Edited by: A. Hofzumahaus

References

Aldener, M., Brown, S. S., Stark, H., Williams, E. J., Lerner, B. M., Kuster, W. C., Goldan, P. D., Quinn, P. K., Bates, T. S., Fehsenfeld, F. C., and Ravishankara, A. R.: Reactivity and loss mechanisms of NO_3 and N_2O_5 in a polluted marine environment: Results from in situ measurements during New England Air Quality Study 2002, J. Geophys. Res.-Atmos., 111, D23S73, doi:10.1029/2006JD007252, 2006.

Allan, B. J., Carslaw, N., Coe, H., Burgess, R. A., and Plane, J. M. C.: Observations of the nitrate radical in the marine boundary layer, J. Atmos. Chem., 33, 129–154, 1999.

Allan, B. J., McFiggans, G., Plane, J. M. C., Coe, H., and McFadyen, G. G.: The nitrate radical in the remote marine boundary layer, J. Geophys. Res.-Atmos., 105, 24191–24204, 2000.

Allan, B. J., Plane, J. M. C., Coe, H., and Shillito, J.: Observations of NO_3 concentration profiles in the troposphere, J. Geophys. Res.-Atmos., 107, 4588, doi:10.1029/2002jd002112, 2002.

Ambrose, J. L., Mao, H., Mayne, H. R., Stutz, J., Talbot, R., and Sive, B. C.: Nighttime nitrate radical chemistry at Appledore island, Maine during the 2004 international consortium for atmospheric research on transport and transformation, J. Geophys. Res.-Atmos., 112, D21302, doi:101.1029/2007JD008756, 2007.

Andrés-Hernández, M. D., Kartal, D., Crowley, J. N., Sinha, V., Nenakhov, V., Martínez-Harder, M., Regelin, E., and Burrows, J. P.: Winter diel peroxy radical concentrations in a semi industrial coastal area: nighttime formation of free radicals, to be submitted to Atmos. Chem. Phys. Discuss., 2011.

Anttila, T., Kiendler-Scharr, A., Tillmann, R., and Mentel, T. F.: On the reactive uptake of gaseous compounds by organic-coated aqueous aerosols: Theoretical analysis and application to the heterogeneous hydrolysis of N_2O_5, J. Phys. Chem. A, 110, 10435–10443, 2006.

Atkinson, R., Baulch, D. L., Cox, R. A., Crowley, J. N., Hampson, R. F., Hynes, R. G., Jenkin, M. E., Rossi, M. J., and Troe, J.: Evaluated kinetic and photochemical data for atmospheric chemistry: Volume I – gas phase reactions of O_x, HO_x, NO_x and SO_x species, Atmos. Chem. Phys., 4, 1461–1738, doi:10.5194/acp-4-1461-2004, 2004.

Atkinson, R., Baulch, D. L., Cox, R. A., Crowley, J. N., Hampson, R. F., Hynes, R. G., Jenkin, M. E., Rossi, M. J., Troe, J., and IUPAC Subcommittee: Evaluated kinetic and photochemical data for atmospheric chemistry: Volume II - gas phase reactions of organic species, Atmos. Chem. Phys., 6, 3625–4055, doi:10.5194/acp-6-3625-2006, 2006.

Badger, C. L., Griffiths, P. T., George, I., Abbatt, J. P. D., and Cox, R. A.: Reactive uptake of N_2O_5 by aerosol particles containing mixtures of humic acid and ammonium sulfate, J. Phys. Chem. A, 110, 6986–6994, 2006.

Bertram, T. H. and Thornton, J. A.: Toward a general parameterization of N_2O_5 reactivity on aqueous particles: the competing effects of particle liquid water, nitrate and chloride, Atmos. Chem. Phys., 9, 8351–8363, doi:10.5194/acp-9-8351-2009, 2009.

Bertram, T. H., Thornton, J. A., Riedel, T. P., Middlebrook, A. M., Bahreini, R., Bates, T. S., Quinn, P. K., and Coffman, D.J.: Direct observations of N_2O_5 reactivity on ambient aerosol particles, Geophys. Res. Lett., 36, L19803, doi:10.1029/2009GL040248, 2009.

Brown, S. S., Stark, H., and Ravishankara, A. R.: Applicability of the steady state approximation to the interpretation of atmospheric observations of NO_3 and N_2O_5, J. Geophys. Res.-Atmos., 108, 4539, doi:10.1029/2003JD003407, 2003a.

Brown, S. S., Stark, H., Ryerson, T. B., Williams, E. J., Nicks, D. K., Trainer, M., Fehsenfeld, F. C., and Ravishankara, A. R.: Nitrogen oxides in the nocturnal boundary layer: Simultaneous in situ measurements of NO_3, N_2O_5, NO_2, NO, and O_3, J. Geophys. Res.-Atmos., 108, 4299, doi:10.1029/2002JD002917, 2003b.

Brown, S. S., Ryerson, T. B., Wollny, A. G., Brock, C. A., Peltier, R., Sullivan, A. P., Weber, R. J., Dube, W. P., Trainer, M., Meagher, J. F., Fehsenfeld, F. C., and Ravishankara, A. R.: Variability in nocturnal nitrogen oxide processing and its role in regional air quality, Science, 311, 67–70, 2006.

Brown, S. S., Dube, W. P., Fuchs, H., Ryerson, T. B., Wollny, A. G., Brock, C. A., Bahreini, R., Middlebrook, A. M., Neuman, J. A., Atlas, E., Roberts, J. M., Osthoff, H. D., Trainer, M., Fehsenfeld, F. C., and Ravishankara, A. R.: Reactive uptake coefficients for N_2O_5 determined from aircraft measurements during the Second Texas Air Quality Study: Comparison to current model parameterizations, J. Geophys. Res.-Atmos., 114, D00F10, doi:10.1029/2008JD011679, 2009.

Carslaw, N., Carpenter, L. J., Plane, J. M. C., Allan, B. J., Burgess, R. A., Clemitshaw, K. C., Coe, H., and Penkett, S. A.: Simultaneous observations of nitrate and peroxy radicals in the marine boundary layer, J. Geophys. Res.-Atmos., 102, 18917–18933, 1997a.

Carslaw, N., Plane, J. M. C., Coe, H., and Cuevas, E.: Observations

of the nitrate radical in the free troposphere at Izana de Tenerife, J. Geophys. Res.-Atmos., 102, 10613–10622, 1997b.

Crowley, J. N., Schuster, G., Pouvesle, N., Parchatka, U., Fischer, H., Bonn, B., Bingemer, H., and Lelieveld, J.: Nocturnal nitrogen oxides at a rural mountain-site in south-western Germany, Atmos. Chem. Phys., 10, 2795–2812, doi:10.5194/acp-10-2795-2010, 2010.

Diesch, J.-M., Drewnick, F., von der Weiden-Reinmüller, S. L., Martinez-Harder, M., and Borrmann, S.: Variability of Aerosol, Trace Gas and Meteorological Characteristics associated with Continental, Urban and Marin Air Masses in the Southwestern Mediterranean, Atmos. Chem. Phys. Discuss., submitted, 2011.

Draxler, R. R. and Rolph, G. D.: HYSPLIT (HYbrid Single-Particle Lagrangian Integrated Trajectory) Model access via NOAA ARL READY Website (http://ready.arl.noaa.gov/HYSPLIT.php), NOAA Air Resources Laboratory, Silver Spring, MD, 2011.

Folkers, M., Mentel, T. F., and Wahner, A.: Influence of an organic coating on the reactivity of aqueous aerosols probed by the heterogeneous hydrolysis of N_2O_5, Geophys. Res. Lett., 30, 1644, doi:10.1029/2003GL017168, 2003.

Fuchs, N. A and Sutugin, A. G.: Highly dispersed aerosols, Ann. Arbor. Sci., Ann. Arbor., 1970.

Geyer, A., Ackermann, R., Dubois, R., Lohrmann, B., Muller, T., and Platt, U.: Long-term observation of nitrate radicals in the continental boundary layer near Berlin, Atmos. Environ., 35, 3619–3631, 2001a.

Geyer, A., Alicke, B., Konrad, S., Schmitz, T., Stutz, J., and Platt, U.: Chemistry and oxidation capacity of the nitrate radical in the continental boundary layer near Berlin, J. Geophys. Res.-Atmos., 106, 8013–8025, 2001b.

Geyer, A., Bachmann, K., Hofzumahaus, A., Holland, F., Konrad, S., Klupfel, T., Patz, H. W., Perner, D., Mihelcic, D., Schafer, H. J., Volz-Thomas, A., and Platt, U.: Nighttime formation of peroxy and hydroxyl radicals during the BERLIOZ campaign: Observations and modeling studies, J. Geophys. Res.-Atmos., 108, 8249, doi:10.1029/2001JD000656, 2003.

Gordon, I. E., Rothman, L. S., Gamache, R. R., Jacquemart, D., Boone, C., Bernath, P. F., Shephard, M. W., Delamere, J. S., and Clough, S. A.: Current updates of the water-vapor line list in HITRAN: A new "diet" for air-broadened half-widths, J. Quant. Spectrosc. Radiat. Transfer, 108, 389–402, 2007.

Griffiths, P. T. and Cox, R. A.: Temperature dependence of heterogeneous uptake of N_2O_5 by ammonium sulfate aerosol, Atmos. Sci. Lett., 10, 159–163, 2009.

Griffiths, P. T., Badger, C. L., Cox, R. A., Folkers, M., Henk, H. H., and Mentel, T. F.: Reactive uptake of N_2O_5 by aerosols containing dicarboxylic acids, Effect of particle phase, composition, and nitrate content, J. Phys. Chem. A, 113, 5082–5090, 2009.

Gross, S. and Bertram, A. K.: Products and kinetics of the reactions of an alkane monolayer and a terminal alkene monolayer with NO_3 radicals, J. Geophys. Res.-Atmos., 114, D02307, doi:10.1029/2008JD010987, 2009.

Gross, S., Iannone, R., Xiao, S., and Bertram, A. K.: Reactive uptake studies of NO_3 and N_2O_5 on alkenoic acid, alkanoate, and polyalcohol substrates to probe nighttime aerosol chemistry, Phys. Chem. Chem. Phys., 11, 7792–7803, 2009.

Heintz, F., Platt, U., Flentje, H., and Dubois, R.: Long-term observation of nitrate radicals at the tor station, Kap Arkona (Rugen), J. Geophys. Res.-Atmos., 101, 22891–22910, 1996.

Hu, J. H. and Abbatt, J. P. D.: Reaction probabilities for N_2O_5 hydrolysis on sulfuric acid and ammonium sulfate aerosols at room temperature, J. Phys. Chem. A., 101, 871–878, 1997.

IUPAC, Subcommittee for gas kinetic data evaluation, (Ammann, M., Atkinson, R., Cox, R. A., Crowley, J. N., Hynes, R. G., Jenkin, M. E., Mellouki, W., Rossi, M. J., Troe, J. and Wallington, T. J.), Evaluated kinetic data: (http://www.iupac-kinetic.ch.cam.ac.uk/,), 2010.

Jensen, N. R., Hjorth, J., Lohse, C., Skov, H., and Restelli, G.: Products and mechanisms of the gas-phase reactions of NO_3 with CH_3SCH_3, CD_3SCD_3, CH_3SH and CH_3SSCH_3, J. Atmos. Chem., 14, 95–108, 1992.

Kane, S. M., Caloz, F., and Leu, M. T.: Heterogeneous uptake of gaseous N_2O_5 by $(NH_4)_2SO4$, NH_4HSO_4, and H_2SO_4 aerosols, J. Phys. Chem. A, 105, 6465–6470, 2001.

Kelly, T. J. and Fortune, C. R.: Continuous monitoring of gaseous formaldehyde using an improved fluorescence approach, Int. J. Environ. Anal. Chem., 54, 249–263, 1994.

Kim, K. H., Jeon, E. C., Choi, Y. J., and Koo, Y. S.: The emission characteristics and the related malodour intensities of gaseous reduced sulfur compounds (RSC) in a large industrial complex, 40, 4478, 2006, Atmos. Environ., 41, 3728–3728, 2007.

Kley, D. and McFarland, M.: Chemiluminescence detector for NO and NO_2, Atmos. Technol., 12, 63–69, 1980.

Martinez, M., Perner, D., Hackenthal, E. M., Kulzer, S., and Schutz, L.: NO_3 at Helgoland during the NORDEX campaign in October 1996, J. Geophys. Res., 105, 22685–22695, 2000.

Mentel, T. F., Sohn, M., and Wahner, A.: Nitrate effect in the heterogeneous hydrolysis of dinitrogen pentoxide on aqueous aerosols, Phys. Chem. Chem. Phys., 1, 5451–5457, 1999.

Merten, A., Tschritter, J., and Platt, U.: Design of differential optical absorption spectroscopy long-path telescopes based on fiber optics, Appl. Opt., 50, 738-754, 2011.

Moise, T., Talukdar, R. K., Frost, G. J., Fox, R. W., and Rudich, Y.: Reactive uptake of NO_3 by liquid and frozen organics, J. Geophys. Res.-Atmos., 107, 4014, doi:10.1029/2001JD000334, 2002.

Mozurkewich, M. and Calvert, J. G.: Reaction probability of N_2O_5 on aqueous aerosols, J. Geophys. Res.-Atmos., 93, 15889–15896, 1988.

Nunes, L. S. S., Tavares, T. M., Dippel, J., and Jaeschke, W.: Measurements of atmospheric concentrations of reduced sulphur compounds in the All Saints Bay area in Bahia, Brazil, J. Atmos. Chem., 50, 79–100, 2005.

Osthoff, H. D., Pilling, M. J., Ravishankara, A. R., and Brown, S. S.: Temperature dependence of the NO_3 absorption cross-section above 298 K and determination of the equilibrium constant for $NO_3 + NO_2 <-> N_2O_5$ at atmospherically relevant conditions, Phys. Chem. Chem. Phys., 9, 5785–5793, 2007.

Pal, R., Kim, K. H., Jeon, E. C., Song, S. K., Shon, Z. H., Park, S. Y., Lee, K. H., Hwang, S. J., Oh, J. M., and Koo, Y. S.: Reduced sulfur compounds in ambient air surrounding an industrial region in Korea, Environ. Monit. Assess., 148, 109–125, 2009.

Platt, U., Lebras, G., Poulet, G., Burrows, J. P., and Moortgat, G.: Peroxy-radicals from nighttime reactions of NO_3 with organic compounds, Nature, 348, 147–149, 1990.

Pöhler, D., Vogel, L., Friess, U., and Platt, U.: Observation of halogen species in the Amundsen Gulf, Arctic, by active long-path

differential optical absorption spectroscopy, P. Natl. Acad. Sci. USA., 107, 6582–6587, 2010.

Riemer, N., Vogel, H., Vogel, B., Anttila, T., Kiendler-Scharr, A., and Mentel, T. F.: Relative importance of organic coatings for the heterogeneous hydrolysis of N_2O_5 during summer, Europe, J. Geophys. Res.-Atmos., 114, D17307, doi:10.1029/2008JD011369, 2009.

Roberts, J. M., Jobson, B. T., Kuster, W., Goldan, P., Murphy, P., Williams, E., Frost, G., Riemer, D., Apel, E., Stroud, C., Wiedinmyer, C., and Fehsenfeld, F.: An examination of the chemistry of peroxycarboxylic nitric anhydrides and related volatile organic compounds during Texas Air Quality Study 2000 using ground-based measurements, J. Geophys. Res.-Atmos., 108, 4495, doi:10.1029/2003jd003383, 2003.

Roberts, J. M., Osthoff, H. D., Brown, S. S., Ravishankara, A. R., Coffman, D., Quinn, P., and Bates, T.: Laboratory studies of products of N_2O_5 uptake on Cl-containing substrates, Geophys. Res. Lett., 36, L20808, doi:10.1029/2009gl040448, 2009.

Rudich, Y., Talukdar, R. K., Ravishankara, A. R., and Fox, R. W.: Reactive uptake of NO_3 on pure water and ionic solutions, J. Geophys. Res., 101, 21023–21031, 1996.

Schuster, G., Labazan, I., and Crowley, J. N.: A cavity ring down/cavity enhanced absorption device for measurement of ambient NO_3 and N_2O_5, Atmos. Meas. Tech., 2, 1–13, doi:10.5194/amt-2-1-2009, 2009.

Shon, Z. H. and Kim, K. H.: Photochemical oxidation of reduced sulfur compounds in an urban location based on short time monitoring data, Chemosphere, 63, 1859–1869, 2006.

Sommariva, R., Pilling, M. J., Bloss, W. J., Heard, D. E., Lee, J. D., Fleming, Z. L., Monks, P. S., Plane, J. M. C., Saiz-Lopez, A., Ball, S. M., Bitter, M., Jones, R. L., Brough, N., Penkett, S. A., Hopkins, J. R., Lewis, A. C., and Read, K. A.: Night-time radical chemistry during the NAMBLEX campaign, Atmos. Chem. Phys., 7, 587–598, doi:10.5194/acp-7-587-2007, 2007.

Sommariva, R., Osthoff, H. D., Brown, S. S., Bates, T. S., Baynard, T., Coffman, D., de Gouw, J. A., Goldan, P. D., Kuster, W. C., Lerner, B. M., Stark, H., Warneke, C., Williams, E. J., Fehsenfeld, F. C., Ravishankara, A. R., and Trainer, M.: Radicals in the marine boundary layer during NEAQS 2004: a model study of day-time and night-time sources and sinks, Atmos. Chem. Phys., 9, 3075–3093, doi:10.5194/acp-9-3075-2009, 2009.

Song, W., Williams, J., Yassaa, N., Regelin, E., Harder, H., Martinez, M., Carnero, J. A. A., Hidalgo, P. J., Bozem, H., and Lelieveld, J.: Characterization of biogenic enantiomeric monoterpenes and anthropogenic BTEX Compounds at a Mediterranean Stone pine Forest site in Southern Spain, to be submitted, J. Atmos. Chem., 2011.

Stutz, J. and Platt, U.: Numerical analysis and estimation of the statistical error of differential optical absorption spectroscopy measurements with least-squares methods, Appl. Opt., 35, 6041–6053, 1996.

Tang, M. J., Thieser, J., Schuster, G., and Crowley, J. N.: Uptake of NO_3 and N_2O_5 to Saharan dust, ambient urban aerosol and soot: a relative rate study, Atmos. Chem. Phys., 10, 2965–2974, doi:10.5194/acp-10-2965-2010, 2010.

Thieser, J., Tang. M. J., Schuster, G., Crowley, J. N., Lelieveld, J., Pöhler, D., Platt, U., and Ganzevelt, L.: Vertical gradients in NO_3 mixing ratios and lifetimes during DOMINO, to be submitted to Atmos. Chem. Phys. Discuss., 2011.

Thornton, J. A., Kercher, J. P., Riedel, T. P., Wagner, N. L., Cozic, J., Holloway, J. S., Dube, W. P., Wolfe, G. M., Quinn, P. K., Middlebrook, A. M., Alexander, B., and Brown, S. S.: A large atomic chlorine source inferred from mid-continental reactive nitrogen chemistry, Nature, 464, 271–274, 2010.

Toda, K., Obata, T., Obolkin, V. A., Potemkin, V. L., Hirota, K., Takeuchi, M., Arita, S., Khodzher, T. V., and Grachev, M. A.: Atmospheric methanethiol emitted from a pulp and paper plant on the shore of Lake Baikal, Atmos. Environ., 44, 2427–2433, 2010.

Vandaele, A. C., Hermans, C., Simon, P. C., Carleer, M., Colin, R., Fally, S., Merienne, M. F., Jenouvrier, A., and Coquart, B.: Measurements of the NO_2 absorption cross-section from 42 000 cm^{-1} to 10 000 cm^{-1} (238–1000 nm) at 220 K and 294 K, J. Quant. Spectrosc. Radiat. Transfer, 59, 171–184, 1998.

Voigt, S., Orphal, J., Bogumil, K., and Burrows, J.P.: The temperature dependence (203-293 K) of the absorption cross sections of O_3 in the 230-850 nm region measured by Fourier-transform spectroscopy, J. Photochem. Photobiol. A-Chem., 143, 1–9, 2001.

Wagner, C., Hanisch, F., Holmes, N., de Coninck, H., Schuster, G., and Crowley, J. N.: The interaction of N2O5 with mineral dust: aerosol flow tube and Knudsen reactor studies, Atmos. Chem. Phys., 8, 91–109, doi:10.5194/acp-8-91-2008, 2008.

Wahner, A., Mentel, T. F., and Sohn, M.: Gas-phase reaction of N_2O_5 with water vapor: Importance of heterogeneous hydrolysis of N_2O_5 and surface desorption of HNO_3 in a large teflon chamber, Geophys. Res. Lett., 25, 2169–2172, 1998.

Wayne, R. P., Barnes, I., Biggs, P., Burrows, J. P., Canosa-Mas, C. E., Hjorth, J., Le Bras, G., Moortgat, G. K., Perner, D., Poulet, G., Restelli, G., and Sidebottom, H.: The nitrate radical: Physics, chemistry, and the atmosphere, Atmos. Env., 25, 1–206, 1991.

Yokelson, R. J., Burkholder, J. B., Fox, R. W., Talukdar, R. K., and Ravishankara, A. R.: Temperature-dependence of the NO_3 absorption spectrum, J. Phys. Chem., 98, 13144–13150, 1994.